Development of a Sustainable, Hybrid Ventilation System

Vaidas Ramelis

Master of Science Thesis

Delft University of Technology

Faculties of Architecture and Aerospace Engineering

Development of a Sustainable, Hybrid Ventilation System

Master of Science Thesis

For the degree of Master of Science in Sustainable Energy Technology at Delft University of Technology

Vaidas Ramelis

May 21, 2015

Wind Energy Research Group · Faculty of Architecture · Faculty of Applied Sciences · Faculty of Aerospace Engineering· Delft University of Technology

The work in this thesis was supported by TNO. Their cooperation is hereby gratefully acknowledged.

Delft University of Technology
Department of
Wind Energy

The undersigned hereby certify that they have read and recommend to the Faculties of Architecture and Aerospace Engineering for acceptance a thesis entitled

Development of a Sustainable, Hybrid Ventilation System

by

Vaidas Ramelis

in partial fulfillment of the requirements for the degree of

Master of Science Sustainable Energy Technology

Dated: May 21, 2015

Supervisor(s): ____________________
Prof. dr. G.J.W. van Bussel

____
Dr. R.M.J. Bokel

____
Ing. B. Knoll

Reader(s): ____________________
Dr.ir. W.A.A.M Bierbooms

Abstract

As building insulation and airtightness are constantly improving, ventilation plays a dominant role in fresh air supply, thermal comfort and managing heat losses and cooling needs. By designing an integrated ventilation system, it is possible to improve air quality and thermal comfort, at the same time enhancing energy efficiency. This thesis focuses on the development of such a ventilation system. It is done by employing the best features of existing systems and including several new features.

Throughout the thesis, ventilation, night cooling, solar shading, heat balance, heat recovery unit and renewable energy sources are studied. In this study, the demanded yearly ventilation air flow rates are found, the optimal heat exchanger model is selected and optimized, yearly energy consumption is calculated, while at the end, a wind cowl is selected and saved yearly energy using the cowl is calculated. The Excel Macro tool is developed and used to establish the needed yearly air flow rates, applying night cooling and solar shading. The Matlab tool is used for the selection and optimization of the heat exchanger as well as yearly energy consumption, with and without the wind cowl. The main specifications of the new system are found. Since a resize of the heat exchanger passage is recommended, an experiment is carried out in order to verify the heat transfer coefficient of the air traveling in the heat exchanger.

The developed ventilation system provides the dwelling with a 'good' indoor air quality at any time of the year, using minimum required air flow rates per room. Thus, combined with the heat recovery device the heating demand for ventilation air is minimized. The system also provides thermal comfort at most times of the year using natural cooling and optimal shading. Thus, the cooling need of the dwelling is minimized. However, due to the heat recovery unit and high night cooling flows, the newly developed ventilation system has an enhanced electricity use. Therefore it is recommended to also redesign the air distribution ductwork system within the dwelling for low pressure use The wind cowl contributes to electricity savings even more if the ventilation system has a well-designed, low pressure air distribution system.

Acknowledgements

I would like to thank my supervisors at Delft University of Technology: Prof. dr. Gerard J.W. van Bussel for his willingness to shear the company contacts he has and time spent while organizing and meeting the members of the TNO research institute, and Dr. Regina M.J. Bokel for her guidance and comments on my progress.

I would like to give my special thanks to my supervisor and engineer at TNO: Bas Knoll for his input and guidance in this project. His experience and knowledge have helped me to gain a fast insight into the ventilation, TNO organization and the research procedure.

I wish to thank the following TNO employees: Karl E. Sewalt, Hans J.C. Phaff, Eric D. Nennie, Piet Jacobs, Bart J. de Boer, Dick H.A.L. van Dijk, Peter de Jong, Wim Kornaat and Henk A.J. Hammink for their guidance and help in the different stages of this project.

Delft, University of Technology | Vaidas Ramelis
May 21, 2015

Table of Contents

List of Figures

List of Tables

List of Symbols

Abbreviations

ATG	Adaptive Thermal Comfort
GBA	Government Buildings Agency
$GOHA$	Government Occupational Health Agency
GTO	Weighted Temperature Exceeding Hours
$KNMI$	Royal Netherlands Meteorological Institute
NTU	Number of Transfer Units
$OECD$	Organization for Economic Co-operation and Development
PMV	Predicted Mean Vote
PPD	Predicted Percentage Dissatisfied
TO	Temperature Exceeding Hours

Greek

ϵ	Ratio of actual transfered heat	-
η	Dynamic viscosity	Pa s
λ	Thermal conductivity	W/(K m)
ω	Relative roughness of duct	-
ϕ	Relative humidity	%
ρ	Density	kg/m^3
ε	Efficiency	%

Latin

A	Surface area	m^2
C_p	Pressure coefficient of cowl	-
c_p	Specific heat capacity	J/(kg K)
$Const$	Constant	-
d	Thickness	m
D_h	Hydraulic diameter	m
dP	Pressure difference	Pa
Dr	Difference between indoor and outdoor humidity	g/kg
f	Friction coefficient	-
H	Height	m
h	Heat transfer coefficient	W/(m^2 K)
L	Length	m
m	Molar mass	kg/mol

P	Total heat production	W
p	Partial pressure	Pa
p_b	Barometric pressure	Pa
p_s	Saturation pressure	Pa
Per	Perimeter	m
$Power$	Power needed for ventilation fan	W
Q	Transfered heat	W
q_p	Volumetric moisture production	m^3/s
q_v	Volumetric flow rate	m^3/s
r	Mixing ratio	-
T	Air temperature	C
t	Time step	s
U	Overall heat transfer coefficient	$W/(m^2\ K)$
V	Volume	m^3
v	Velocity	m/s
X	Stack's Constant	-
z_f	Friction coefficient	-
z_o	Landscape roughness length	m

Subscripts

a	Air
$chan$	Heat exchanging channel
$cross$	Cross-sectional
$design$	Pre-determined design value
EL	Electricity
$exch$	Heat exchange
h	Heat
he	Heat exchanger
in	Indoor
$in-1$	Previous step indoor
$in1$	Indoor before heat exchanger
is	Indoor storage
$iwall$	Indoor walls
Mat	Material
NG	Natural gas
out	Outdoor
$out1$	Outdoor before heat exchanger
$out2$	Outdoor after heat exchanger
Pl	Plastic after recast
ref	Reference value

Sp Space
$summer$ Warm season when heat exchanger is not used
$time$ Time when heat exchanger is used
$vent$ Ventilation
w Water
$wall$ Storage
$wall-1$ Previous step storage
$wall1$ Inner wall
$wall2$ Outer wall
$wind$ Windows
$windsun$ Windows facing sun

Chapter 1

Introduction

In the 21-st century, people are becoming increasingly aware of the depletion of conventional energy sources, greenhouse problems and a steadily growing human population. Since human nature does not want to reduce its comfort, the responses to these challenges are: a transition to renewable energy and an increased efficiency of the existing systems. The energy statistics of *OECD* countries shows that from 30 to 50 % of primary energy is used in non-industrial buildings [1]. A significant portion of this energy is dissipated from the building in the exhausted air stream. Since buildings are becoming more thermally insulated, air ventilation becomes the dominant heating and a cooling loss mechanism in a building [2]. For these reasons, it is crucial to enhance the energy efficiency of ventilation. On the other hand, health complaints related to poor indoor air quality occur in approximately 15% of Dutch houses [3], while the excess heat is either poorly controlled or removed using electricity demanding air conditioners. Because of this, air quality and thermal comfort of a house needs to be improved as well.

1-1 Conventional Ventilation Systems

Natural ventilation with exhaust duct
It is the most popular ventilation system in the Netherlands. It consists of naturally driven air supply and mechanically driven exhaust. In general, the fan of the exhaust system can run at three speed levels. Only the highest speed level meets the minimum ventilation demands of the Dutch building regulations. Lower speed levels are meant for use during periods in which dwellers are not at home. Air inlet openings in outer walls consist of ventilation grids. Air outlets are found in a kitchen, a toilet and a bathroom and consist of a valve connected with the exhaust tube system that leads to the exhaust fan situated at the roof level [4]. This system can deliver three different demand controlled flow rates with relatively low pressure drops. However, it has huge heat losses since the exhaust heat is not regained. Moreover, the extracted air flow is well controlled, whereas the incoming flow distribution in a building is almost incontrollable and depends on the wind, temperature differences and the altitude of a building.

Balanced heat recovery ventilation
Mechanically driven supply and exhaust ventilation systems with heat recovery are found in houses built in the last decade. This system offers a good energy saving potential, also introduces fresh air to a building and improves climate control. In this system, the counter-current, air-to-air heat exchanger is used. The supply and extraction fans are used in order to force the air to move into ducts and through the heat exchanger. In this system, air distribution in a building is well controlled for every room, energy is saved by recovering heat and the heat exchanger is a compact unit. However, since the heat exchanger consists of small heat exchanging channels which can eventually be blocked by even small particles, high density filters are used to filter the smallest particles. Due to the small size of the channels and dense filters, the system results in large pressure drops at high flow rates. Moreover, at a high vapor production in the house, water clogging may occur in the heat exchanger, making the pressure drop even higher.

The conventional ventilation systems are usually driven by mechanical fans which are not efficient and increase electricity use even further. Neither of the systems can provide an excess heat control in the warm season. Therefore, when using these systems, the overheating of the dwelling is prevented by window airing, creating high natural flows at night or the use of an air conditioner. Yet, window airing is not burglar-free, consequently, it increases robbery risks. An air conditioner consumes a lot of electricity. The schemes of the both systems are shown in figure 1-1.

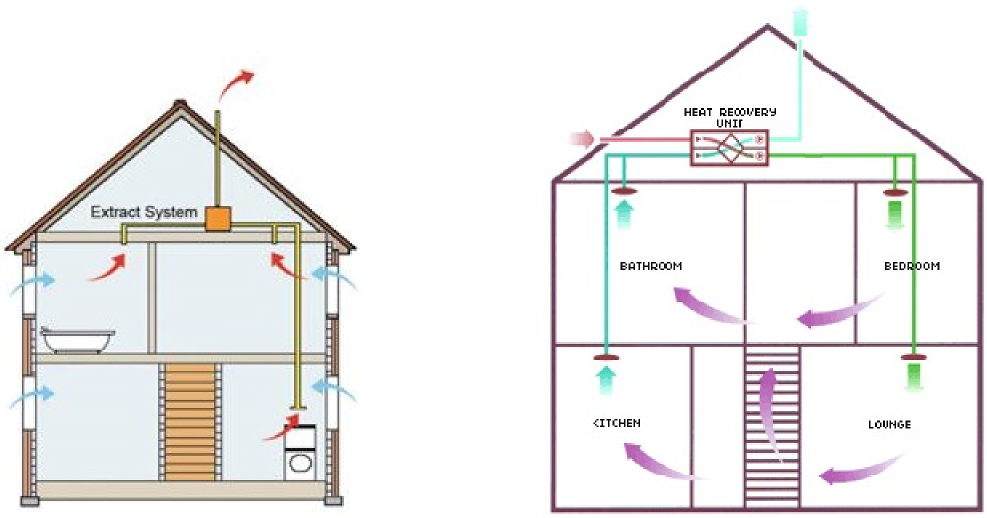

Figure 1-1: Ventilation system with exhaust unit (left). Balanced ventilation with heat recovery (right).

1-2 Requirements for New System

Knowing problems related to conventional ventilation systems, it is possible to eliminate them completely or reduce in the upcoming systems. In this research, an attempt is made to create a system which has the best parts of present systems and eliminates or diminishes their shortages. The requirements for the new system are mentioned below.

1. Two functions should be combined in one system, enabling low pressure heat recovery in winter and enhanced, well controlled air flow rates in summer. For cooling purposes, higher flow rates, bypassing the heat exchanger, could also be used in some parts of the dwelling in the heating season.

2. The system should provide the required air flow rates which dilute the dominant contaminant to the acceptable level. The dominant contaminant could vary depending on a season.

3. Water clogging in the heat exchanger should be avoided. Condensed water blockage can increase pressure drop up to a few times. In winter, water may freeze, reducing air passage to the minimum, hence, condensed water should be removed before it blocks the heat exchanger.

4. The system should be easy to clean and use lower density filters. Denser filters cause higher pressure drop, which in turn results in greater electricity consumption, especially if larger air flow rates are used.

5. Renewable sources should be used in order to reduce the energy consumption of the system. The needed electricity can be reduced by using wind cowls. Yet, the profitability of the cowl and saved energy part should be determined before using it.

6. The system should distribute the demanded controlled air flow rates into different rooms. Air flow rates should be increased when occupants are present and diminished when occupants are not in their dwelling. The flow rates should also be distributed within the dwelling, e.g. the total air flow should be delivered to bedrooms at night, while living rooms should be most intensively ventilated during the day.

1-3 Research Goal

The main goal of this research is to determine the specifications of the new ventilation system (flow rates, energy consumption, size, preliminary cost) which fulfilling the requirements mentioned in 1-2:

1. provides a well-insulated house, located in the Netherlands climate zone, with an acceptable air quality and thermal comfort at most times of the year;

2. is as energy efficient as possible. It includes heating, cooling losses and electricity consumption.

1-4 Approach Overview

In order to accomplish the main research goal, firstly, the two mentioned conditions have to be fulfilled, not forgetting the system's requirements. Since the house under consideration is well-insulated, a ventilation system plays the major role supplying fresh air and ensuring an acceptable indoor temperature. Thus, the first step is to find ventilation air flow rates which are required to provide the house with a 'good' air quality and a sufficient thermal comfort. In order to restrain the needed flow rates in summer, night cooling and solar shading techniques were applied. After the necessary flow rates were determined, the next step is the investigation of the medium which accommodates the flow rates. In order to minimize heat losses in winter, a heat exchanger is used. The size of the heat exchanger channels is considerably bigger than that of conventional systems. Larger channels prevent condensed water blockage, since water can drain down the duct. It is also easier to clean, requires lower density filters and creates lower pressure drop, which means lower electricity consumption. However, an increased size of the channels also results in a reduction of heat transfer efficiency. Therefore, the heat exchanger's size and geometry have to be adjusted to reach the optimum between efficiency and pressure drop. Since the heat exchanger is not used and higher flow rates are required in summer to maximize the use of natural cooling, bypassing ducts were incorporated to reduce electricity consumption. Next to it, the ventilation system switches to the exhaust mode, where both air passages are used for the extraction of the air combined with natural supply openings through burglar free grids. At the end, different wind cowls were investigated in order to determine which part of the needed power could be provided by the wind cowls.

1-5 Thesis Outline

The thesis is organized as follows:

- **Chapter 2** describes theory which is needed to understand the basics of ventilation, heat recovery unit and wind cowls. It also gives a short description of a few techniques which were studied but due to their shortcomings are not included in this research. Some parts of this chapter present some reasoning, if it is needed, why certain techniques were chosen to proceed with. The main steps in determining ventilation flow rates, heat exchanger's efficiency and pressure drop are presented as well.

- **Chapter 3** presents a calculation of the ventilation air flow rate which is needed to ensure a 'good' air quality and thermal comfort. At the beginning of this chapter, using various graphs, the needed air flow rate for odor control is determined. Then, air flow rates for the humidity removal are determined. Afterwards, a heat balance is made and the required flow rates for excess heat control, including solar shading and night cooling, are established. At the end, final flow rates for the whole year are defined.

- **Chapter 4** introduces a recovery unit of the ventilation system. Firstly, four different heat exchanger variations are investigated. Then, judging on the total price, the best option is selected. Afterwards, the optimum dimensions based on efficiency, pressure drop, taken space and used materials are determined. Finally, a whole year energy calculation, including regained heat and used electricity, is computed.

- **Chapter 5** presents an experiment which was carried out during the research. At the beginning, the chapter describes the tested heat exchangers' production sequence. Then, the experiment's setup is presented. At the end, results are shown and comparisons with computed values are displayed.

- **Chapter 6** indicates which part of energy can be saved by using the wind cowl. At the beginning of this chapter, different cowls are investigated. Then, the best performing cowl is selected. Afterwards, upper and lower boundary cases are made to estimate the unknown performance of the cowl when wind speed is lower than the air velocity in the ventilation duct. At the end, the both cases are compared and the total energy savings are calculated.

Chapter 2

Theory

In this chapter, a short overview of the theory which was used in the research is introduced. The material presented in this chapter is meant to guide the reader through the chosen research path. It also familiarizes readers, with the basics which are needed to understand further research development. Several techniques which were studied but not used are presented as are the reasons prevented them to be exploited. Since it is a multidisciplinary study involving ventilation, heat recovery and wind energy studies, several assumptions were made in order to simplify this study and save time. Although most of the assumptions are presented in further sections, a couple of them presented below.

1. Outdoor air quality is considered to be perfect. Clearly, the outdoor air also contains many pollutants, such as traffic fumes, fungi, agricultural chemicals, pollen, industrial pollutants, noise, methane, radon etc. Nevertheless, it is assumed that the house under consideration is located in an area where these pollutants are at neglectable concentrations.

2. The density of the air is assumed to be constant. Since air density depends on temperature and the temperature under the consideration is in a range of -12 and $+32.5$ degrees Celsius, the air density for this research ranges from 1.35 to 1.15 (kg/m^3). The value of $1.25 kg/m^3$ is chosen for further calculations.

2-1 Ventilation

Ventilation is needed to provide oxygen for metabolism and remove metabolic pollutants (carbon dioxide and odor) from people in the house. It is also used to maintain a 'good' air quality in the house, by diluting and removing other pollutants, e.g. moisture. Frequently, the dominant pollutant is heat itself, then ventilation, applying different techniques, can be employed for house cooling.

The amount of the required ventilation depends on the quantity and nature of the pollutants in the house. Usually, there are countless numbers of different pollutants in houses. Figure 2-1 (a) presents some pollutants which can be found in a house [5, 6, 7].

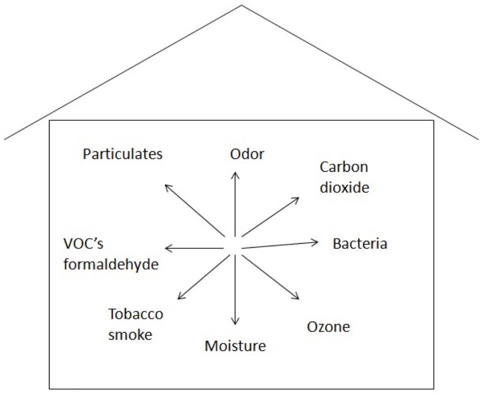

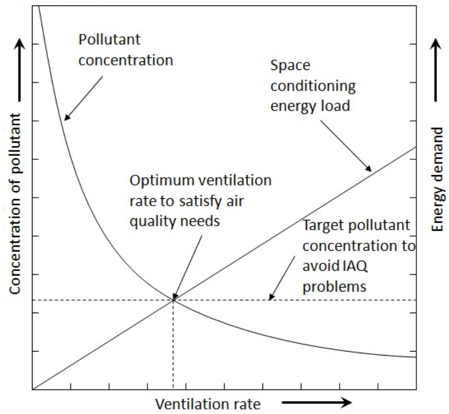

Figure 2-1: a) Overview of typical indoor pollutants (left); b) Control of dominant pollutant (right)

If the emission characteristics of each contaminant are known, it is possible to calculate amount of ventilation needed to prevent each pollutant from exceeding a pre-defined threshold concentration. However, many of the pollutants are at almost immeasurably low concentrations and have largely unknown toxicological effects. Therefore, in order to determine the total needed ventilation, it is useful to identify the dominant pollutant. Provided that the sufficient ventilation rate is used to control the dominant pollutant, all the remaining pollutants should stay below their respective threshold concentrations. As a result, the minimum acceptable ventilation rate is that which is needed to dilute the dominant pollutant to an acceptable concentration. Figure 2-1 (b) shows the relationship between pollutant concentration, ventilation rate and energy load [8, p. 5].

Controlling Indoor Air Pollutants

Table 2-1 presents the summary of pollutant control order and methods.

Source control: If pollutants enter a house, at best, they can only be diluted. Therefore, avoidable pollution sources, such as smoking, should be removed from the house.

Method	Pollution source
Source control	Emissions from avoidable sources (formaldehyde from furnishings, tobacco smoke etc.)
Ventilation at source	Pollutants generated by occupant activities (cooking, clothes washing, use of office equipment, combustion apparatus etc.)
Dilution ventilation	Emission from unavoidable sources (metabolism pollution)

Table 2-1: Preferred methods to control indoor pollutant sources

Ventilation at source: Pollutants which are generated by occupants' activities, such as washing, clothes drying, cooking, are usually localized in a certain room or room area. Source ventilation should be applied wherever possible by using local extractors, a cooker or range hoods.

Dilution ventilation: General ventilation of a space is needed to dilute and remove residual pollution from unavoidable contaminant sources. Such sources are primarily odors and carbon dioxide emissions from occupants. A necessity to keep metabolic pollution to acceptable levels represents the minimum need for ventilation [8, p. 29].

Philosophy behind the ventilation demands in Dutch building regulations is that ventilation should only take account for the removal of substances that can not be prevented to penetrate the indoor air, such as carbon dioxide, water vapor and bio effluents that result from human activity and physiological processes. Chemicals of building materials and furniture should be avoided or their emissions should be reduced to prevent concentration levels that can harm human health [4]. Since thermal comfort is one of the system's requirements, excess heat should also be accounted for. As a result, assuming that avoidable pollutants are not the case and both cooking and combustion contaminants are removed at source by placing the cooker hood, a particular attention in this research is paid for carbon dioxide, odor, humidity and heat control of the house. Hence, further sections of this chapter describe the path in which the needed volumetric air flow rates, which are required for the control of these contaminants, are calculated.

2-2 Ventilation for Odor Removal

Metabolic odors create discomfort and often indicate poor indoor air quality, but a problem related to the odor is that it is not possible to measure odor intensity with any instrumentation. Therefore, there have been several attempts to measure odor intensity by other means. Yaglou considered the occupants' impact on odor intensity [9, p 423-435]. Professor P.O. Fanger also examined the building itself as a pollution source [10] and created his well known indoor air quality units of measuring ('Olf' and 'decipol') to quantify the building's odor intensity [11].

2-2-1 Fanger's Method and its Shortcomings

Professor Fanger suggested that odor intensity should be judged by visiting 'panelists'. The main units introduced to odor analysis are the 'Olf', which is an odor emission rate from a 'standard' person, and the 'decipol', which is the intensity of odor or 'perceived' air quality derived from a source of one 'Olf' ventilated by $10dm^3/s$ of fresh air. 'Olf' emission from other sources, such as building materials, are expressed in terms of emission from one standard person (a one-Olf source). Thus, this method can be used in order to determine a ventilation flow rate which is needed to minimize odor discomfort. Implicit to this method is the assumption that odor from different sources can be summed to obtain the total odor value, although types of odor may differ.

However, this method has one disadvantage which is why it was not used in this study. It is almost impossible to tell at a design stage what odor intensity from other than occupant's metabolism sources, such as furnishing, fittings, will be. It also differs from house to house.

2-2-2 Metabolic Odor Intensity Relation to CO_2 Concentration

Another way to determine the ventilation flow rate for odor control is carbon dioxide concentration. Metabolism related odor intensity from occupants is linked to CO_2 concentration [12]. In other words, the increase of CO_2 concentration in the house results in the increased metabolic odor intensity. Extensive experiments show that the number of complaints increases significantly at CO_2 levels above 1200 ppm. Thus, to avoid odor nuisance CO_2 levels should not exceed 1200 ppm. [13]. Yet, in order to achieve the A quality level of indoor air, only 10% of dissatisfaction is allowed [8, 31p.]. CO_2 concentration can either be measured by carbon dioxide sensors or calculated from occupants' activities. Knowing CO_2 concentration, it is possible to find the required volumetric flow rate to dilute carbon dioxide concentration to an acceptable level. The required ventilation flow rate can be determined by performing the following steps:

1. The average metabolic rate is determined for every occupant of the house, depending on age and activity. It is done by using table 2-2

	Metabolism	
Activity	W/m^2	met
reclining, sleeping	46	0.8
seated relaxed	58	1
standing at rest	70	1.2
sedentary activity (office, dwelling, school)	70	1.2
standing light activity (shooping, light industry)	93	1.6
standing, medium activities (shop asistant, domestic work)	116	2
Domestic work - washing by hand and ironing	170	2.9

Table 2-2: Metabolic rate and produced heat dependence on a person's activity [14]

2. The average carbon dioxide production rate, which dependents on age and average metabolic rate, is determined for every occupant. It is done by using figure 2-2.

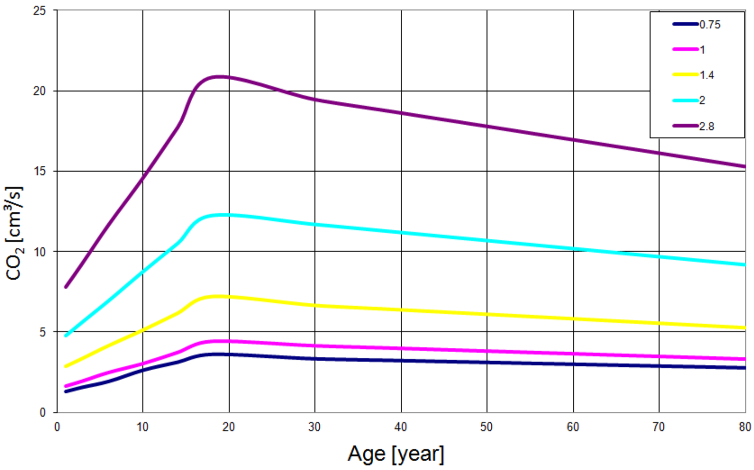

Figure 2-2: CO_2 production dependence on age and metabolic rate [15]. Legend presents met values

3. Using Bouwman's plot, the percentage of acceptability is checked. In order to achieve 90% of satisfaction, indoor carbon dioxide concentration must be around 800 ppm.

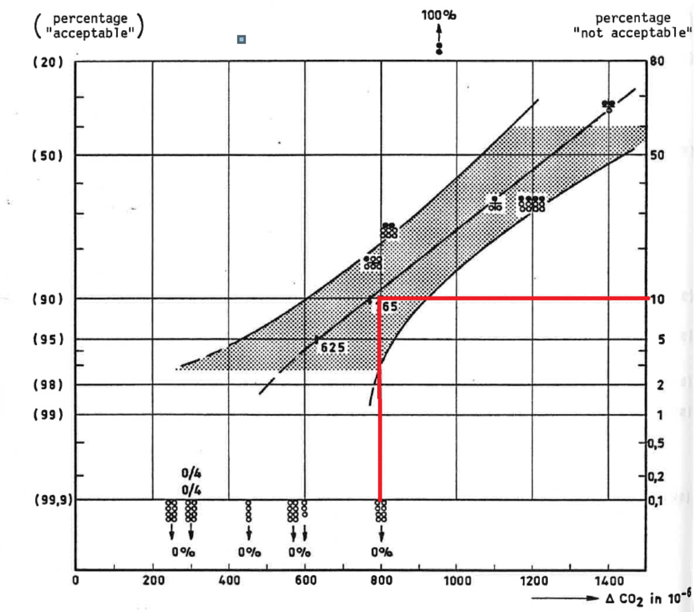

Figure 2-3: Acceptability dependence on CO_2 concentration [12]

4. Then the required air flow is found by dividing the average carbon dioxide pro-

duction rate by indoor CO_2 concentration. See the following equation:

$$Requiredflowrate = \frac{CO_2production}{CO_2concentration} \tag{2-1}$$

Although odor intensity does not always have a direct and strict relation to CO_2 and Bouwman's plot has wide margins, this method is chosen since it does not require special skills. Afterwards, it is checked whether the calculated air flow rate does not contradict to the minimum ventilation flow rate standards [16].

2-3 Ventilation for Humidity Removal

Low humidity can lead to discomfort, like dry tissues of nose, mouth and eyes, shrinkage of wood floors and wood furniture, cracking of paint on wood trim and static electricity discharges. On the other hand, high humidity can lead to problems with molds, corrosion, decay and other moisture related deterioration. In extreme cases, water condensation can occur on cold surfaces. If the level of humidity in the air exceeds a certain level, it leads to fungus and bacteria growth [17]. These organisms can only survive if the temperature and relative humidity of the air are within certain limits. For fungi and bacteria that are commonly found indoors, the optimum temperature and the humidity percentage range from 0 to 35°C and 70 to 95% respectively [18, 835p.]. Because of this, the indoor level of relative humidity should never be higher than 70 %.

The humidity level of an indoor space can be described through relative humidity. **Relative humidity:** the ratio of the actual water vapor pressure of the air to the saturated water vapor pressure of the air at the same temperature expressed as a percentage [19]. In simple words, it is the ratio of the current mass of moisture in the air in relation to the mass at 100% moisture in the air, at a given temperature. The relative humidity is expressed as a percentage and is given in equation 2-2.

$$\phi = \frac{p_w}{p_{s,w}} 100\% \tag{2-2}$$

According to ASHRAE 62-2001 standards, people feel 'good' when relative humidity is between 25 - 60% [16]. However according to other studies, relative humidity should be between $30-70\%$ [20]. The latter values have been chosen for this research. Although it is possible that indoor relative humidity drops below thirty percent, that occurs rarely. On the other hand, high relative humidity, especially under wet mid-season conditions and at high humidity production, occurs quite often. In order to prevent moisture related problems, humidity has to be removed from the house via a ventilation system.

The required air flow rate is determined by the following steps.

1. Knowing the temperatures of the indoor and outdoor air, it is possible to calculate saturated water vapor pressures. It is done by using experimentally determined

equations [21]. Equation 2-3 is used for temperatures above zero Celsius degrees and equation 2-4 for temperatures below zero Celsius degree.

$$\log p_{s,w} = 10.8(1-\frac{273}{T})-5\log(\frac{T}{273})+1.5{\cdot}10^4(1-10^{-8.3(\frac{T}{273}-1)})+4{\cdot}10^4(10^{4.8(1-\frac{273}{T})}-1)-0.2 \tag{2-3}$$

$$\log p_{s,w} = -9.1(\frac{273}{T}-1) - 3.6\log(\frac{273}{T}) + 0.9(1-\frac{T}{273}) - 0.2 \tag{2-4}$$

Note: due to its length, the equations were shortened to tenths after the decimal point.

2. Then, the air mixing ratio is calculated for both environments using equation 2-5

$$r_a = \frac{m_w p_{s,w}\frac{\phi}{100\%}}{m_a(p_b - p_{s,w}\frac{\phi}{100\%})}[22] \tag{2-5}$$

3. Thereafter, the difference between two air mixing ratios Dr is found by subtracting one from the other.

4. If the humidity production rate by the occupants q_p and the air mixing ratio difference between indoor and outdoor air are known, a volumetric flow rate which is needed to control the humidity level is found. It is done with equation 2-6.

$$q_{v,a} = \frac{q_p}{Dr\rho_a} \tag{2-6}$$

2-4 Ventilation for Temperature Control

In a residential house, heat gains come from occupants, solar radiation, high outdoor temperature, lighting, household apparatus and other electrical sources. In warm season, these factors make the cooling of the indoor air essential. In this research, house cooling is done by introducing higher ventilation flow rates at night (when the outdoor air is cooler than the indoor air) and reduced flow rates during the day (when the outdoor air is warmer than the indoor air). In order to minimize solar load, solar shading devices are used.

The first question which has to be answered is: what temperature is comfortable? Thermal sensations play a key role in the perception of comfort and, as other comfort parameters, are highly subjective. Moreover, thermal comfort depends on several variables, such as air temperature, outdoor wind speed, metabolic rate of occupants, clothing etc. In order to answer the raised question, Dutch guidelines for thermal comfort are used. There has been three successive methods in the Netherlands for the design, simulation and assessment of thermal comfort in buildings [23]. These methods are described below.

PMV and Temperature Exceeding Hours(TO)

In 1979, the GBA and GOHA agreed that a 'good' thermal indoor climate had to comply with -0.5 < Predicted Mean Vote < 0.5, based on the Predicted Mean Vote - Predicted Percentage of Dissatisfied relation [24]. These limits are allowed to be exceeded to the maximum -1.0 < PMV < 1.0 for no more than ten percent of the occupied time, only under exceptional circumstances. These basic agreements were further developed by the GBA in the Temperature Exceeding Hours method. This method stated that temperature in a dwelling may exceed 25°C no more than one hundred hours a year, whereas 28°C may exceed no more than 10-20 hours a year. The climate year 1964-1965 was chosen as a standard year for the temperature simulations. This climate year was considered to be a moderate year in terms of temperature, so in a warmer year more exceeding hours were to be accepted.

Weighted Temperature Exceeding Hours (GTO)

Temperatures are likely to be higher in buildings having a lighter thermal mass than in heavier buildings with a higher thermal mass. Therefore, dissatisfaction will be lower in heavier buildings. Yet, this effect is not considered in the TO method. This is why, in 1989 the Weighted Temperature Exceeding Hours method was introduced in the Guidelines for Governmental Buildings. In this method, hours during which the calculated or actual PMV exceeds a PMV-limit of +0.5 are weighted proportional to the PPD. Thus, the temperature that results in a PPD of 20 % during one hour will be weighted twice as severe as the temperature that results in 10% dissatisfied. When the PMV has a value of 0.5 (PPD=10) the weighting factor is one. When the PMV has a value of one (PPD=26) the weighting factor is 2.6 (see table 2-3).

PMV	PPD	Weighting factor
0	5	0
0.5	10	1.0
0.7	15	1.5
1.0	26	2.6

Table 2-3: PMV,PPD and weighting factor

On the basis of computer simulations, it was found that the number of hours, when indoor temperature exceeds 25°C, should be lower for lighter buildings, whereas for heavy buildings without air-conditioning, the GTO guidelines correspond quite well with the TO. Summarized results of the GTO method are given in table 2-4.

Building mass[1]	Free running	Air-conditioned
Extremely light	70 to 85	< 95
Medium light	80 to 95	< 115
Heavy	90 to 110	< 115

1

- Extremely light: wooden floors/ceilings, light walls (thermal mass <5 kg/m^2)
- Medium light: concrete floors/suspended ceilings, light walls (thermal mass approx. 50 kg/m^2)
- Heavy: heavy concrete floors/open ceilings, heavy walls (thermal mass approx. 100 kg/m^2)

Table 2-4: Hours exceeding 25°C at 150 GTO hours (weighted temperature exceeding hours PMV>0.5)

Knowing the thermal mass of a building, the possible number of hours exceeding 25°C is determined.

Adaptive Temperature Limits (ATG)

It was found that in sealed, centrally air-conditioned buildings where occupants have no option to open windows, the adaptability to a changing temperature was very limited [25], whereas in naturally ventilated buildings with operable windows and ceiling fans the occupants' adaptability was considerably higher. In the Netherlands, the abstract terms *Alpha* and *Beta* were introduced to characterize distinct building types and a flow chart was developed to distinguish between these two situations (the chart can be found in [23]). The allowable operative indoor temperature dependency on the weighted outdoor temperature for the both building types is shown in figures 2-4 and 2-5.

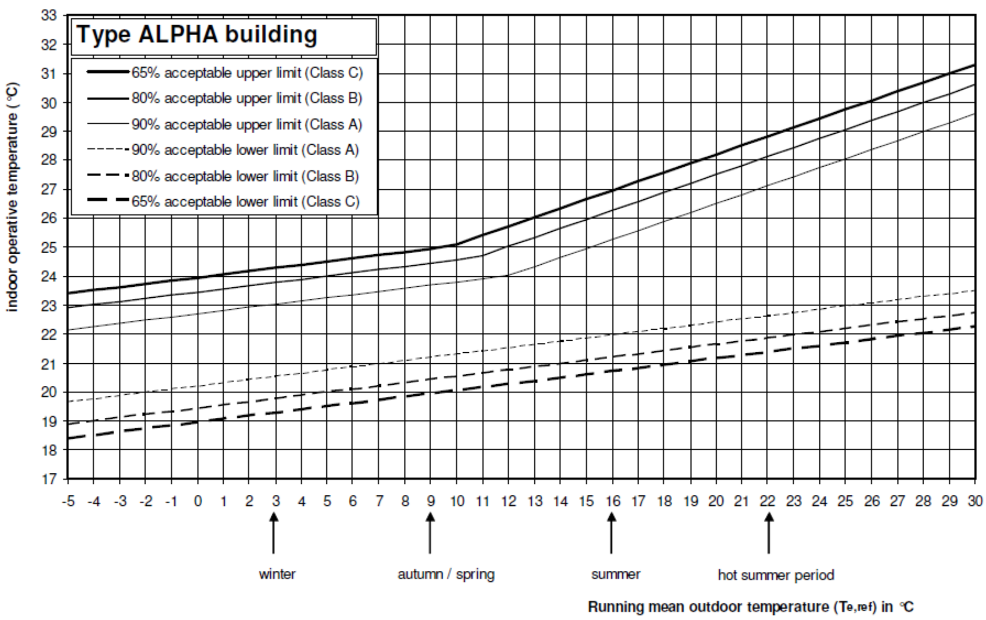

Figure 2-4: Building type *Alpha*. Limits of operative indoor temperatures, as a function of weighted outdoor temperature

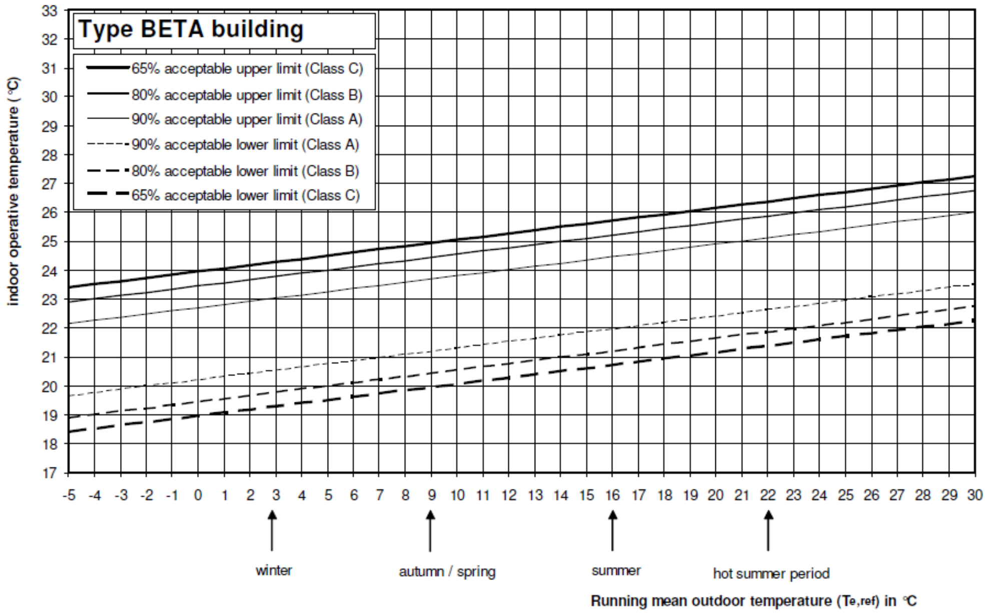

Figure 2-5: Building type *Beta*. Limits of operative indoor temperatures, as a function of weighted outdoor temperature

Following new guidelines, it is assumed that a 'good' climate is characterized by 80% of acceptance. In other words, it is required that a building's performance never exceeds the limit values for 80% of acceptance at specified outdoor climate.

In one study [23], it was found that in order to comply to the (ATG) limits, the required cooling capacity has to be doubled to eliminate a minor amount of exceeding hours. As a consequence, the ATG method is rejected. Since in order to use the Weighted Temperature Exceeding hours method, the exact thermal mass of a building should be known, the GTO method is also rejected. Consequently, the TO method is chosen for this research.

2-4-1 Heat Balance for House

For an hourly temperature calculation purpose, a very simplified heat balance is used which is given in international standards (ISO 13790:2008(E)) annex B[26]. The heat balance includes conductive heat transfer through a building's walls and windows, convective heat transfer through a ventilation system, heat fluxes to and from the thermal mass of walls and the indoor air, outdoor and indoor temperatures, and internal as well as solar heat sources. The graphic presentation of the heat balance is shown in figure 2-6.

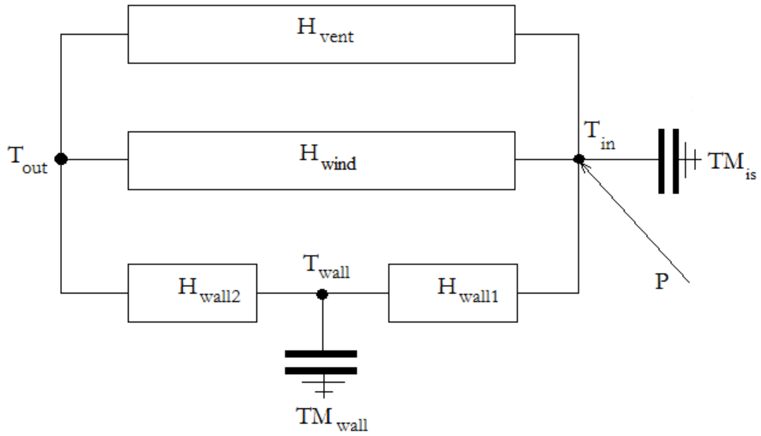

Figure 2-6: Heat balance of house

In equation 2-7, the principle of the heat balance is shown.

$$heat_{incoming} + heat_{production} = heat_{outgoing} \tag{2-7}$$

If a building's characteristics as well as solar and outdoor temperature data are known then the heat balance can be constructed. Equations 2-8 and 2-9 show the heat balance which was constructed according to figure 2-6.

$$H_{vent}(T_{in} - T_{out}) + H_{windows}(T_{in} - T_{out}) + H_{wall1}(T_{in} - T_{wall}) + \frac{TM_{is}}{t}(T_{in} - T_{in-1}) = P \tag{2-8}$$

$$H_{wall1}(T_{wall} - T_{in}) + \frac{TM_{wall}}{t}(T_{wall} - T_{wall-1}) + H_{wall2}(T_{wall} - T_{out}) = 0 \tag{2-9}$$

Where:

$H_{vent} = q_{v,a} c_{p,a} \rho_a$

$H_{wind} = U_{wind} A_{wind}$

$H_{wall1} = U_{wall1} A_{wall}$

$H_{wall2} = U_{wall2} A_{wall}$

$TM_{is} = \rho_{wall} c_{p,wall} V_{iwall}$

$TM_{wall} = \rho_{wall} c_{p,wall} V_{wall}$

In order to calculate the ventilation needed flow rate to keep the acceptable indoor temperature, these equations are reorganized and solved.

2-5 Heat Recovery Unit

The heat recovery unit or, in this specific case, the air-to-air counter-current heat exchanger has two important parameters: heat transfer efficiency (further efficiency) and pressure drop. The first parameter indicates the percentage of heat which is regained from the outflowing air. Pressure drop, basically, corresponds to the energy which is consumed while driving the air though the heat exchanger. While a higher efficiency is a desirable goal, pressure drop is an unwanted side effect. Since every attempt to increase efficiency, almost in all cases, results in a higher pressure drop as well, a careful design of the heat exchanger is needed. Therefore, a good design requires the optimum between high efficiency and the acceptable pressure drop values.

2-5-1 Efficiency Calculation Using NTU Method

This section presents a short description of the Number of Transfer Units method, used to calculate the efficiency of the heat exchanger. Since the NTU method is very wide, it can be used for calculations of many different heat exchangers. First of all, the equations were adjusted to the air-to-air, counter-current, even in-/outflow heat exchanger. Only the most important steps and equations of the NTU method are given in this section. An extensive reasoning behind every equation can be found in [27, ch. 2.6].

1. Three separate parameters are determined: the heat transfer surface area, the overall heat transfer coefficient and incoming/outgoing air magnitudes. The heat transfer surface area depends only on the geometry and size of the heat exchanger and its channels, thus, it can be calculated using only logical reasoning. The overall heat transfer coefficient represents the sum of all heat transmission rates involved. This is expressed as:

$$\frac{1}{U} = \frac{1}{h_a} + \frac{d_{chan}}{\lambda_{chan}} + \frac{1}{h_a} \tag{2-10}$$

   Note: the heat transfer coefficient of the incoming and outgoing air flows (h) is slightly different. However, since the air flow rates are equal, this value is taken to be even. It simplifies the calculations. The explanation of the overall heat transfer coefficient and the main problems determining it are given in subsection 2-5-2. The incoming/outgoing air magnitudes represent the heat transmission rate dependency on the air properties and the volumetric flow rate. This is defined as:

$$H_{vent} = q_{v,a}\rho_a c_{p,a} \tag{2-11}$$

2. The number of transfer unit is determined. This unit takes into account all the three parameters explained above. This is expressed as:

$$NTU = \frac{A_{exch}U}{C} \tag{2-12}$$

3. The Non-dimensional ratio of the actual heat transfer rate ϵ is found. Knowing that both outgoing and incoming ventilation flow rates are equal, the equation can be very simplified:
$$\epsilon = \frac{NTU}{1 + NTU} \tag{2-13}$$

4. The actual amount of the transfered heat is found using the following equation:
$$Q = \epsilon C(T_{in1} - T_{out1}) \tag{2-14}$$

5. Since the total transfered heat is already known, it is possible to calculate outflowing air temperature after it exits the heat exchanger (air temperature which is incoming to the indoor). This is expressed as:
$$T_{out2} = \frac{Q}{C} + T_{out1} \tag{2-15}$$

6. At the end, the temperature efficiency of the heat exchanger is calculated:
$$\varepsilon = \frac{(T_{out2} - T_{out1})}{(T_{in1} - T_{out1})} 100\% \tag{2-16}$$

   It should be noted that the heat exchanger's temperature efficiency can also be calculated by finding outgoing indoor air temperature after the air passes the heat exchanger (the temperature of the air which is exhausted to the outdoor environment).

2-5-2 Overall Heat Transfer Coefficient

The overall heat transfer coefficient is presented by equation 2-10. It represents the sum of three heat transmission rates: from the outgoing air to the heat exchanger's wall ($1/h_a$), through the wall itself (d_{chan}/λ_{chan}), from the heat exchanger's wall to the incoming air ($1/h_a$). All the three heat transmission mediums are shown in figure 2-7.

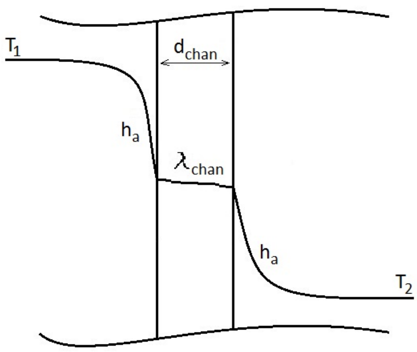

Figure 2-7: Heat transmission chain air-wall-air

Due to small thickness, heat transfer through the heat exchanger's wall is negligible. Therefore, the material used for the heat exchanger's production has very little influence on the overall heat transfer coefficient. On the other hand, heat transmissions through the air play the major role in the overall heat transfer coefficient. Since air flow rates in the heat exchanger are equal, the air-wall and wall-air heat transfer coefficients are considered to be equal.

Overall Heat Transfer Coefficient Problem

The heat transfer coefficient through solid materials is well known. However, as it has been already mentioned in section 2-5-2, the overall heat transfer coefficient mainly depends on the air-wall and wall-air heat transmission coefficients. Hence, these values have to be determined with high accuracy. Unfortunately, although it is well known that the air-to-wall (wall-to-air) heat transfer coefficient is very dependent on air velocity, hydraulic diameter and heat exchanger's length, there are several distinct theoretical equations found in literature to calculate it [28, p. 75],[29, p. 150-152]. The calculated values are diverse. There are several empirical equations found in literature as well [29, p. 153]. Still, it is not clear which of them should be used since the results differ from one study to another. Figure 2-8 shows the heat transfer coefficient dependency on air velocity, assuming that the length of the heat exchanger and the height of the channels are 1 and 0.015 meters respectively.

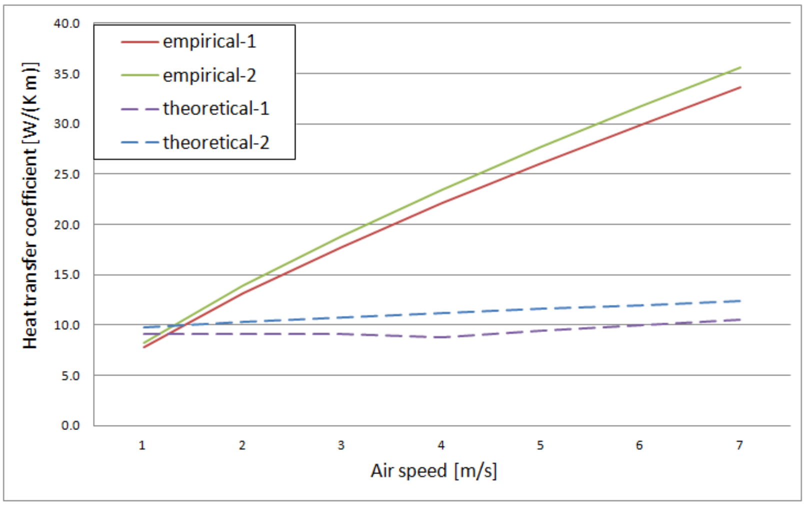

Figure 2-8: Heat transfer coefficient dependency on air velocity. '$empirical-1$' and '$empirical-2$' are taken from [29, p. 153], '$theoretical-1$' and '$theoretical-2$' are taken from [29, p. 152] and [28, p. 75], respectively

As it can be seen in figure 2-8, a general trend is that the heat transfer coefficient increases with the increase of air velocity. However, the heat transfer values which are computed by using the empirically determined equations have a much steeper slope than the ones from theoretically established equations. '$empirical - 1$' also takes into account the average temperature between the outdoor and indoor air, whereas

'$empirical - 2$' assumes a constant value instead. The empirically determined equations are more trustworthy since they are based on measured data, so the theoretical equations are rejected. Since the average temperature between the outdoor and indoor air will change depending on a month and a season, the decision is made to follow the empirically determined equation (equation 2-17) for the heat transfer coefficient calculation ('$empirical - 2$' in the graph).

$$h_a = 4.4 \frac{{v_a}^{0.75}}{{D_{h,chan}}^{0.25}} \tag{2-17}$$

2-5-3 Pressure Drop Calculations

As it was mentioned in section 2-5, pressure drop through the heat exchanger is also a very important parameter. So, it must be considered when designing a heat exchanger. This section presents the main steps which are needed in order to determine pressure drop across the heat exchanger. An extensive reasoning behind every equation can be found in [27, ch. 4].

1. The cross-sectional area of the heat exchanger and the hydraulic diameter of the heat exchanger's channels are calculated. As for the heat transfer surface area, the cross-sectional area depends only on the geometry and size of the heat exchanger and its channels. As a consequence, it can be calculated by using logical reasoning. The hydraulic diameter of the channels, on the other hand, can be found by using a general equation:
$$D_{h,chan} = \frac{4A_{chan}}{Per_{chan}} \tag{2-18}$$

2. Given a uniform velocity profile, air velocity in the heat exchanger is found as follows:
$$v_a = \frac{q_{v,a}}{A_{cross}} \tag{2-19}$$

3. The Reynolds Number is found by using the following equation:
$$Re = \frac{v_a D_{h,chan} \rho_a}{\eta_a} \tag{2-20}$$

4. Using the Reynolds Number and assuming that channels of heat exchangers are very smooth, the Darcy-Weisbach friction factor (f_a) is found. The friction factor dependency on the Reynolds Number and the relative roughness of the channels are depicted in the Moody diagram. It is shown in figure 2-9. The friction factor for a laminar flow region is calculated by using the following equation:
$$f_a = 64/Re \tag{2-21}$$

In order to approximate the friction factor in a turbulent flow region, several equations were examined by calculating friction factor values and comparing them with one another. The Swamee-Jain equation is chosen because it is easy to use and calculated values are very close to the real ones. The equation is shown below:

$$f_a = 0.25(\log_{10}(\frac{\omega}{3.7} + \frac{5.74}{Re^{0.9}}))^{-2} \tag{2-22}$$

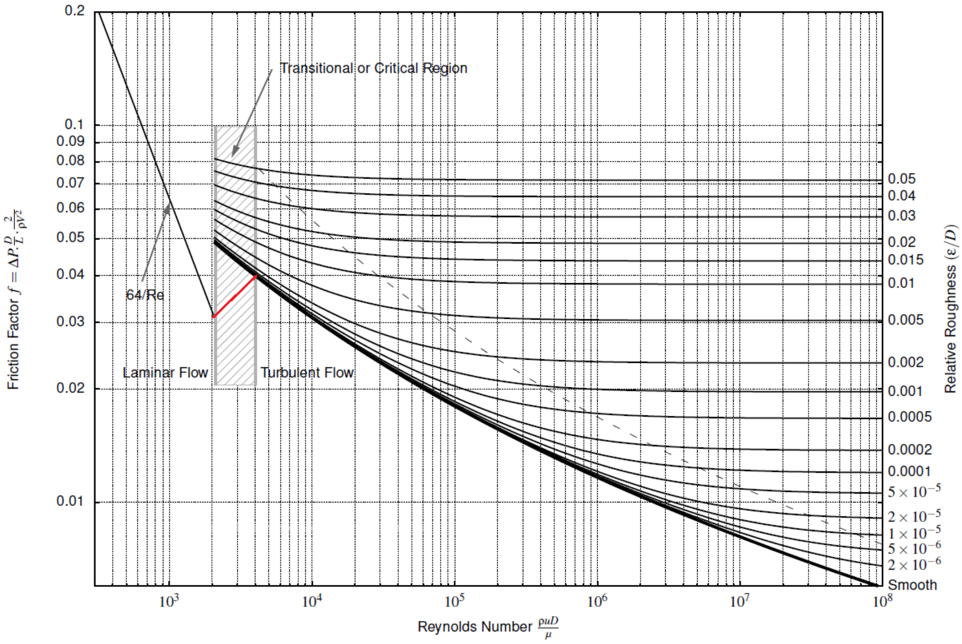

Figure 2-9: Moody diagram

The friction factor is almost unpredictable in a transitional (or critical) region. Even though, there are several ways to estimate the friction factor in this region.

- extend either the laminar or turbulent flow lines (in the figure 2-9, turbulent flow lines are extended);
- extend the both flow lines up to they meet in the halfway;
- connect the ends of the two flows with a straight line.

In this research, the third option is chosen (red line in figure 2-9). The expression which connects the two lines is given in the equation below:

$$f_a = 0.010522 + \frac{0.01279Re}{1700} \tag{2-23}$$

5. At the end the pressure drop is calculated by using the following equation:

$$dP = \frac{f_a L_{he} \rho_a {v_a}^2}{2D_{h,chan}} \tag{2-24}$$

In addition to the pressure drop of the heat exchanger, filters and other ducts also induce a relatively high pressure drop. If pressure drop of filters and the ductwork is known at a certain design air flow rate, then pressure drop of other flow rates for the same system can be calculated using equation 2-25.

$$dP_{design} = Const * {q_{v,a}}^2 \tag{2-25}$$

Firstly, the constant ($Const$) is found by using the known design values. Then pressure drop of other flow rates can be calculated.
If fan efficiency, the pressure drop of ductwork, the heat exchanger and filters are known, the power needed to drive the fan can be found using the following equation:

$$Power = \frac{q_v dP}{\varepsilon_{fan}} \tag{2-26}$$

2-5-4 Stack Effect

When temperature indoor is higher than outdoor, due to a difference in the air density, a positive pressure difference is established between the inside and outside of a dwelling. The positive pressure difference forces the air to rise. In the reverse case, a negative pressure difference increases the air suction in a dwelling. This air transport phenomenon, due to the air density, is called the stack effect. It reduces the pressure drop through the ductwork in winter. However, it may increase ventilation resistance in summer, when air temperature indoor is lower than outdoor. Pressure differences created due to the stack effect depend on the height of a dwelling, indoor and outdoor air temperature difference and the atmospheric pressure. The induced pressure difference is calculated using the following equation.

$$dP = Xp_bH(\frac{1}{T_{out}} - \frac{1}{T_{in}}) \tag{2-27}$$

Here X=0.0342

2-6 Wind Cowls

The wind, perpendicularly flowing above the open tube which is located on top of the roof, creates lower pressure at the opening fo that tube. It causes pressure difference between the two ends of the tube, inducing the suction force and air flow through the tube towards the rooftop. By changing the shape of the tube's opening, which faces the wind, it is possible to increase pressure difference between the two ends. Moreover, by placing the cowl on the tube, pressure difference can increase even more. The cowl also offers protection from rain and birds' nests. Nevertheless, the cowl also increases the resistance for the air flowing along the tube. Therefore, the increase of pressure difference, due to the cowl, should be weighed against extra resistance which is created by the cowl.

2-6-1 Wind Data

In most natural terrains, the surface of the earth is not uniform and changes significantly from location to location. Wind speed is sensitive to terrain roughness. Wind speed reduces with the increase of terrain roughness. It is classified by using surface roughness length [30, 44 p.]. Different classifications are shown in table 2-5.

Type of terrain	Roughness length z_o (m)
Flat desert, rough sea	0.001
Flat grassy plains	0.01
Open farmland, a few trees and buildings	0.03
Villages, countryside with trees and hedges	0.1
Suburbs, wooded countryside	0.3
Cities, forests	0.7

Table 2-5: Surface roughness length for different terrains

Wind speed also depends on height. The wind speed dependency on height and surface roughness describes the wind profile, which is shown in figure 2-10.

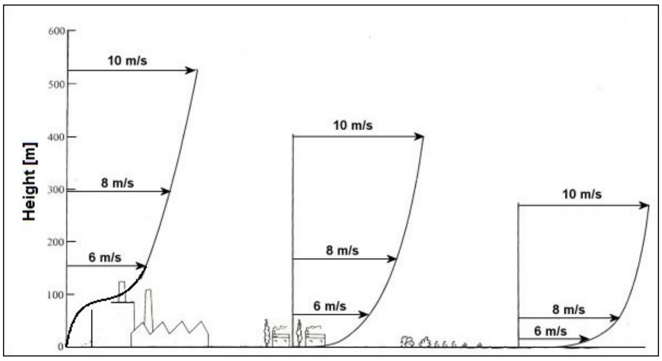

Figure 2-10: Wind profile at different terrains

Using the wind profile with the surface roughness area, wind speed at a certain height can be found from the logarithmic law equation 2-28.

$$v_{wind}(H) = v_{wind}(H_{ref})\frac{ln(H/z_o)}{ln(H_{ref}/z_o)} \tag{2-28}$$

2-6-2 Wind Cowl Resistance and Suction Force

As it has already been mentioned, an additional cowl increases the resistance of an outlet duct. This mainly depends on the shape and placement of the cowl. Cowl resistance is expressed as a friction coefficient (z_f) for flows through tube systems. Some values of friction coefficients can be found in [28, 83p.] or [29, 254p.]. Then, pressure drop, including wind cowl, is found by using equation 2-29.

$$dP = \frac{\rho_a {v_a}^2}{2}(z_f + f_a \frac{L_{he}}{D_{h,chan}}) \tag{2-29}$$

The suction force or pressure difference, created by the cowl, is calculated by using equation 2-30 [31, 165p.].

$$dP_{cowl} = C_p \frac{1}{2} \rho_a {v_{wind}}^2 \tag{2-30}$$

The cowl pressure coefficient (C_p) depends on the type of the cowl and can by determined experimentally. S.Toet performed experiments with three different pipe opening shapes and two wind cowls in the wind tunnel at Delft University of Technology. The wind was applied perpendicularly to the openings and the cowls [32]. In an other extensive study by W.F.de Gids and L. den Ouden, fourteen different cowls were examined in wind tunnel. This study included various vertical angles from which the wind was approaching cowls [33]. The study showed that the vertical wind angle from which it approaches the cowl is crucial for the cowl's pressure coefficient.
However, A. Pfeiffer, V. Dorer and A. Weber performed a study, where, by using computational fluid dynamics, a few separate cases were investigated. In the first case, it was assumed that the pressure coefficient is only a function of wind speed and air velocity in the duct ratio. Hence, a zero degree vertical angle was chosen (perpendicular to the cowl). In another case, the pressure coefficient was carefully calculated including the localized vertical angle of the approaching wind. The results were very similar, but the second case took much more efforts to compute [34]. Based on A. Pfeiffer, V. Dorer and A. Weber's study, the pressure coefficient, in the present research, is calculated assuming that the wind is approaching a cowl perpendicularly. The cowl with the best pressure coefficient is selected for further calculations.

Chapter 3

Air Flow Rates Required for New System

In this chapter, the following question is answered: what flow rates are required to ensure the acceptable indoor air quality and a thermal comfort? The required flow rates are calculated for metabolic odor, carbon dioxide, humidity and excess heat control.

The required flow rates for odor and CO_2 removal are determined by using the 2-2, 2-3 figures and simple mathematical expressions. Microsoft Office Excel 2010 is used for humidity control calculations. Flow rates for excess heat removal, including night cooling and solar shading, are simulated using VBA Macros 2010. Hourly temperature, pressure, relative atmospheric humidity at 1.5 meters height and wind speed (at 10 meters) data used in the simulations, are taken from the Royal Netherlands Meteorological Institute. The data are taken for the entire year of 2013 at Rotterdam meteorological station No. 344.

3-1 House data

Since the approximate size of a house and indoor air and wall volumes are required for heat balance simulations, a 'Tussenwoning' type concrete house, which was build in 1992-2005 and has C energy-index, is chosen for this research. It is assumed that the residents' family consists of four people: two adults (30-35 years old) and two children (3 and 10 years old). The house layout is shown in figure 3-1. In the layout, the house characteristics are approximated. Windows', walls', roof's surface areas as well as the air and walls' volumes are estimated by using the mathematical expressions (complete calculations can be found in appendix A).

Figure 3-1: 'Tussenwoning' house type, scale 1:200

The thermal heat transfer coefficients through the windows, the outer wall envelope, the roof and the floor are taken from [35, p. 44-45]. The concrete and air properties are taken from [28, p. 114-117],[36] and [37]. It is assumed that the floors and the indoor walls thermal transfer coefficients are equal. In order to introduce the thermal mass of the building into the simulations, the outer walls are divided into two layers. The outer layer is made of pre-cast concrete and has high thermal insulation. On the other hand, the inner part (which is 0.1 m thick) has higher thermal transfer coefficient (foam concrete), resulting in elevated heat intake and outtake speeds. The indoor walls are assumed to be 0.05 m thick and have the same thermal transfer coefficients as the inner layer of the outer walls. Every window which is located on the south side of the house has the outdoor louvers which act as a solar shading. Louvers uncoil if solar irradiation reaches a certain value. Table 3-1 presents determined house characteristics.

Building's characteristic	Notation	Value	Units
total window area	A_{wind}	19	m^2
total windows exposed to sun area	$A_{windsun}$	11	m^2
total house carcass wall area	A_{wall}	180	m^2
total house carcass wall volume	V_{walls}	25.9	m^3
total indoor walls and floor volume	$V_{insidewalls}$	12.5	m^3
total indoor air volume	$V_{insideair}$	328	m^3
total house envelope area	$A_{houseenvelope}$	262	m^2
windows' heat transfer coefficient	U_{wind}	2.9	$\frac{W}{m^2K}$
outer walls' heat transfer coefficient	U_{wall2}	0.4	$\frac{W}{m^2K}$
inner walls' heat transfer coefficient	U_{wall1}	6.2	$\frac{W}{m^2K}$
density of wall	ρ_{wall}	2160	$\frac{kg}{m^3}$
specific heat capacity of wall	$c_{p,wall}$	1130	$\frac{J}{kgK}$
specific heat capacity of air	$c_{p,a}$	1006	$\frac{J}{kgK}$

Table 3-1: House characteristics

3-2 Air Flow Rate for Odor Control

Carbon dioxide itself has recorded harmful effects on human' health only at high levels. However, as it has already been mentioned in section 2-2-2, metabolic odor intensity is related to carbon dioxide concentration. Increasing CO_2 concentration, odor intensity is also enhanced. As a result, if CO_2 is kept at a certain predetermined level, metabolic odor heaviness also stays at the acceptable level.
The needed ventilation flow rates based on CO_2 control are found by using the steps given in 2-2-2. It is hardly possible to accurately estimate people activity levels in the house. As a result, rough assumptions are made. It is known that the family consists of four people of different age (3,10 and 30 years). It is assumed that, on average, adults spend most of their time doing light or medium light activities. A younger child also does average intensity activities, while an older child does more intense activities. Hence, by using table 2-2, metabolic rates of the children and the adults were determined: $1.4met$ for the younger child and the adults, and $1.6met$ for the older child.
Then, according to figure 2-2, carbon dioxide production is determined with respect to

metabolic rate and age. It is $6.5cm^3/s$ for the adults, $4cm^3/s$ for the three years old child and $7cm^3/s$ for the older child (10 years). The total CO_2 production is $24cm^3/s$. Figure 3-2 presents carbon dioxide production depending on age and averaged activities.

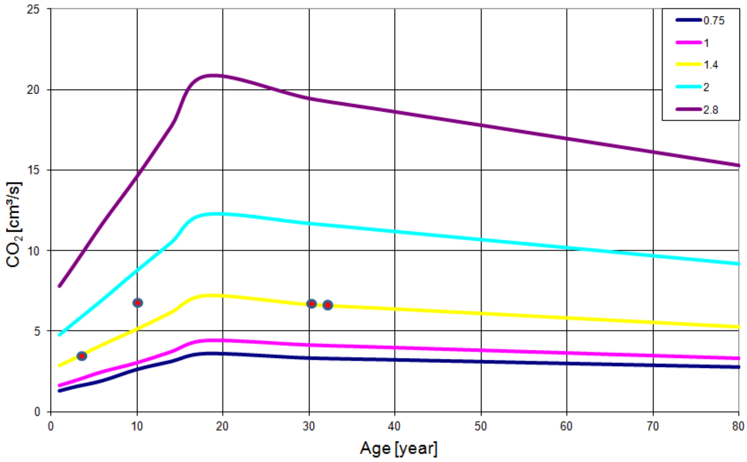

Figure 3-2: CO_2 production from separate persons depending on age and activity level

Then, a volumetric flow rate which is needed to remove the CO_2 production of the individuals is found.

$$q_{v,CO_2} = \frac{CO_{2,production}}{CO_{2,acceptableconcentration}} = \frac{0.024dm^3/s}{800ppm}1000000 = 30dm^3/s \qquad (3\text{-}1)$$

In order to validate the calculations, the obtained flow rate is compared to the Netherlands regulations for dwellings [38] which note that the minimum of $7dm^3/s$ per person is required. After the flow rate is multiplied by the number of occupants, it becomes $28dm^3/s$. Hence, a minimum flow rate of $30dm^3/s$ is acceptable.
Clearly, the older child has to go to the school and at least one of the adults has to go to work. As a consequence, it is possible to reduce the ventilation flow rate during different parts of the day, by employing user patterns. However, as this requires extensive knowledge of family habits and obligations, this it is not included in the present research.

3-3 Air Flow Rate for Humidity Control

In order to avoid moisture related problems, the relative humidity of the dwelling is not allowed to exceed 70 %. The excessive moisture is removed through a ventilation system. If the system is not able to cope with humidity on some summer days, a dehumidifier could be employed. Nevertheless, the ventilation system should be able to remove excessive humidity for most of the year.
A study made by the TNO (the study is based on [39]), found that the average four people family produces around 10 dm^3 of moisture a day. The study includes moisture production from different sources, such as showering, drying of the clothes, mopping

the floor, people themselves etc. A percentage division of moisture production by its source is shown in figure 3-3.

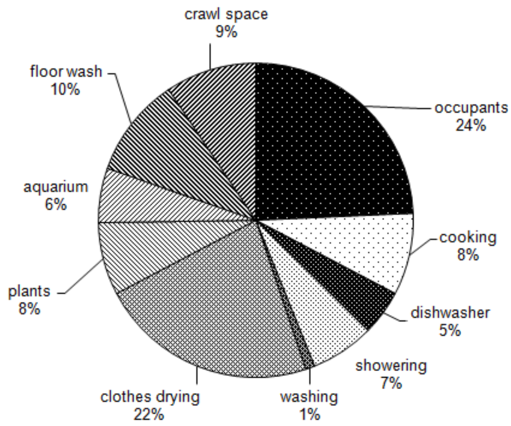

Figure 3-3: Moisture production by its source expressed in percentage

For the purpose of simplicity it is assumed that the building's heating system keeps the indoor temperature at 19.7°C at any time of the day. According to a habitants survey, 19.7°C is the most preferable dwelling temperature in the Netherlands [40]. In warm season, indoor temperature will become higher. Therefore, the following equation is used to estimate indoor temperature, if outdoor air temperature exceeds 17.7°C.

$$T_{in} = T_{out} + 2\exp(-\frac{T_{out} - 17.7}{3}) \tag{3-2}$$

Equation 3-2 presents the empirically determined indoor temperature dependence on outdoor temperature [41]. Note that this equation is used only for humidity control. Knowing outdoor hourly temperature and relative humidity from the KNMI as well as indoor temperature, relative humidity limit and moisture production, the required flow rates for humidity control are calculated following the steps mentioned in section 2-3. First of all, the saturated water vapor pressure of indoor and outdoor temperatures are calculated for every hour of the year. The outdoor saturated water vapor pressure is calculated by using both equations 2-3 and 2-4, depending on the temperature sign. Then air mixing ratios are calculated. Thereafter, hourly difference between two air mixing ratios is found. In order to reduce fluctuations, 12 hours is chosen as the average time. In the end, the required hourly ventilation flow rate, depending on the moisture production rate and the humidity average difference between indoor and outdoor, is calculated.

3-3-1 Humidity Control Scheme

After hourly calculations for the whole year are done, it appears that the ventilation system can cope with excessive humidity in the cold period of the year. Yet, in some

days of the warm year period, the outdoor air moisture level is almost the same as that of the indoor air. In this case, the ventilation would need to have very high flow rates to remove excessive humidity. When the indoor air mixing ratio is approaching the outdoor level, a certain maximum ventilation flow rate value has to be established to avoid very high flow rates. On the other hand, there are some time periods when indoor humidity is lower than outdoor (e.g. raining and morning mist).
The moisture level is satisfied when indoor relative humidity is equal to or lower than 70%. The maximum flow rate is determined by finding the optimum between the applied maximum flow rates and the number of hours, expressed in percentage when the humidity level is satisfied. This is shown in figure 3-4.

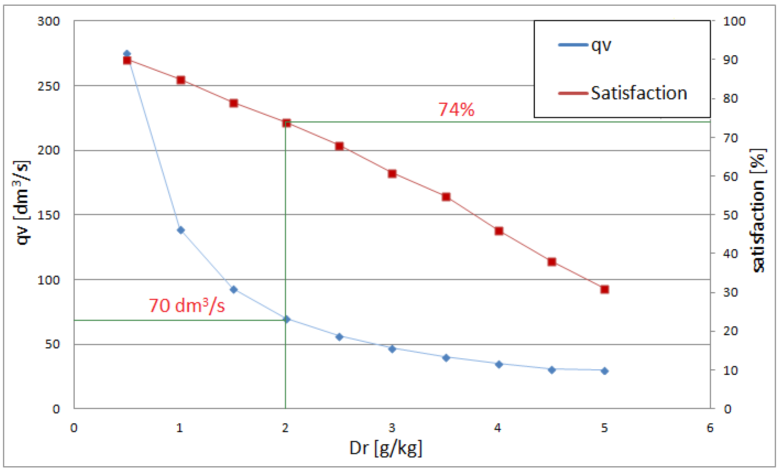

Figure 3-4: Applied maximum ventilation flow rates and humidity level satisfaction

With regard to the above graph, the flow rate of 70 dm^3/s, which satisfies 74 % of the whole year, is considered to be the optimum and is chosen to be the maximum flow rate. When the outdoor moisture level is higher compared to the indoor, the ventilation is reduced to the lowest possible flow rate. A moisture flow rate control scheme is presented next.

- **If** the difference in the moist air mixing ratio between indoor and outdoor is higher than 2 g/kg, **then** the ventilation is determined by hourly calculations.
- **If** the difference in the moist air mixing ratio between indoor and outdoor is lower than 2 but higher than 1 g/kg, **then** the maximum ventilation flow rate of 70 dm^3/s is applied.
- **If** the difference in the moist air mixing ratio between indoor and outdoor is lower than 1 g/kg, **then** the air flow rate is reduced to zero.

Applying the maximum and minimum values, the hourly ventilation flow rates of the whole year are shown in figure 3-5.

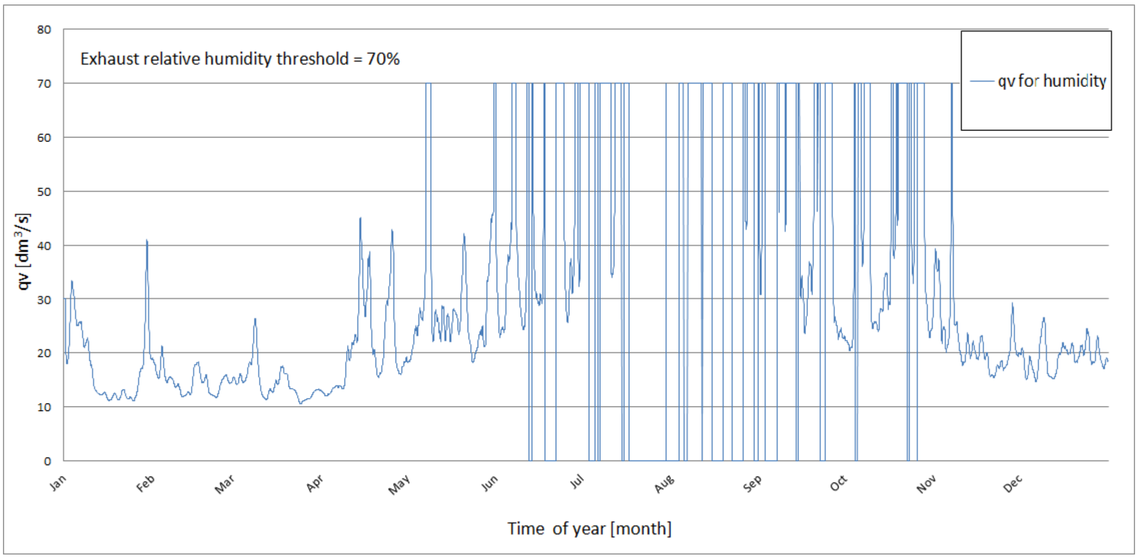

Figure 3-5: Required flow rates for moisture control

In order to check if flow rates are realistic, they are compared with the results of the TNO research [41]. In the same conditions, the results of both the TNO research and this study are similar. A comparison can be found in appendix B.

3-4 Air Flow Rate for Excess Heat Control

It is obvious that an excessive heat problem occurs only in the hot period of the year. Thus, only three hottest months, from June 11th to September 10th, are simulated. The simulations are based on a heat balance which is defined by equations 2-8 and 2-9. It is computed on the minutely basis by using Microsoft Excel, VBA Macros 2010. House characteristics, used in the heat balance, are taken from table 3-1. There are two types of solar shading investigated in this research: single glass windows with indoor louvers (heat permeability is 45 %) and double windows with outdoor louvers (heat permeability is 15 %) [42, p. 10]. Solar shading is applied whenever solar irradiation reaches a certain value. The optimum value is determined during the simulations.

Heat Gains

Heat gains of the house are threefold: the main heat gain from solar radiation, gains from electric equipment and part of heat from the house occupants when they are in the house. This is presented in equation 3-3.

$$P = P_{solar} + P_{electricity} + P_{occupants} \tag{3-3}$$

If solar shading is applied, solar gain is multiplied by heat permeability, depending on solar shading type.

Heat gain from electricity equipment is calculated by dividing the average annual electricity use in the Netherlands by the number of hours per year.

$$P_{electricity} = \frac{3500000(W/year)}{8760(hours/year)} = 399W \tag{3-4}$$

Heat gain from the occupants is calculated by using the user patterns of the average four people family [43]. Tables 3-2 and 3-3 show how much time, in hours, the occupants spent in different rooms. It also presents metabolic rate and emitted heat (per m^2) for various activities.

	bedroom	**living room**	**kitchen**	**bathroom**	**out of house**
man	7	5.25	0.25	0.5	11
woman	7	12	1.5	0.5	3
10 years child	11	2.25	0.25	0.5	10
3 years child	12.25	8	0.25	0.5	3
metabolism	0.8	1	1.2	1.2	–
$\frac{W}{m^2}$	46	58	70	70	–

Table 3-2: Families' patterns (hours present) during working days and average metabolic activity in different rooms

	bedroom	**living room**	**kitchen**	**bathroom**	**out of house**
man	9	11.25	0.25	0.5	3
woman	9	10.5	1	0.5	3
10 years child	11.75	8.5	0.25	0.5	3
3 years child	12.75	7.5	0.25	0.5	3
metabolism	0.8	1	1.2	1.2	–
$\frac{W}{m^2}$	46	58	70	70	–

Table 3-3: Families' patterns (hours present) during weekend and average metabolic activity in different rooms

Table 3-4 presents the size of the skin depending on the age of a person.

person	**skin size [m^2]**
man	1.7
woman	1.7
10 years child	1.4
3 years child	1.2

Table 3-4: Skin size of different persons. [44, p. 2457]

Knowing the averaged skin size, time spent inside the house and metabolic activities of the occupants (expressed in W/m^2), the total daily heat production is calculated by multiplication. The final result is given in table below.

person	**produced heat during working days [W]**	**produced heat during weekend [W]**	**average[W]**
man	48	79	63.5
woman	82	80	81
10 years child	40	63	51.5
3 years child	54	54	54
total	224	276	**250**

Table 3-5: Average heat production from occupants

The average heat production by the four occupants is 250 W.

3-4-1 Heat Balance Control Scheme

Excess heat is calculated on the basis of heat balance. However, since night cooling and solar shading are applied, a certain control scheme is needed. The control scheme consists of the following steps for every hour:

1. Solar irradiation, volumetric flow rate (which is taken from the odor and humidity control results), current and forecasted outdoor temperatures are read from the file. Initial indoor and storage temperatures are assigned.
2. If solar irradiation is bigger than a certain predefined value, solar shading is applied.

3. The total heat gain is calculated.
4. If the forecasted temperature is higher than the certain predefined value, night cooling is applied, i.e. the air flow rate is increased to the maximum. The maximum air flow rate value is freely chosen. If night cooling is applied, steps 5 and 6 are skipped. The cooling mechanism is explained in section 3-4-2.
5. The indoor and storage temperatures are computed by using the heat balance for every minute of the hour. In the end, temperature values are averaged.
6. The heat balance equations are rearranged and the ventilation air flow rate is adjusted to get the wanted indoor temperature. This is done by following these steps:
   - if indoor temperature is lower than 25°C, then an air flow rate is controlled by humidity;
   - if indoor temperature is higher than 25°C and outdoor temperature is lower than 25°C, then an air flow rate which lowers the indoor temperature to 25°C is calculated;
   - if indoor and outdoor temperatures are higher than 25°C, then an air flow rate is decreased to minimum ($30 dm^3/s$) in order to reduce heat gains from the outdoor air.
7. New indoor and storage temperatures are calculated by using the obtained air flow rates.

It should be noted that in practice the ventilation controller will follow the aforementioned steps.

3-4-2 Night Cooling

A night cooling mechanism switches on if the forecasted outdoor temperature of the coming day reaches a certain predefined value. Clearly, this value has to be somewhere in between 20 and 25°C. If the maximum ventilation switched on when the forecasted outdoor temperature is lower than 20°C, it would result in high energy consumption and a fan would have to work on the full load very frequently. On the other hand, if the maximum air flow rate switched on when the forecasted outdoor temperature is higher than 25 °C, it would result in higher than 25 °C indoor temperature in the future. However, there are too many variables to be checked, therefore, for this research, the forecasted outdoor temperature value is chosen to be constant, i.e. 22°C.
Another constant is the time slot of the forecasted temperature. It is taken to be 11 hours. The $KNMI$ data show that outdoor temperature reaches its peak around 11 a.m. and 1 p.m., whereas the lowest point is around 11 p.m. and 1 a.m. Temperature is already very high around 9 a.m. and calculating 11 hours backwards would be 10 p.m., when outdoor temperature is almost at the lowest point. Using these considerations, the forecasted temperature time slot of 11 hours is a reasonable choice.

Using these two predefined constants, the following night cooling scheme is defined for every hour:

1. If outdoor temperature in an 11 hours period reaches 22°C or night cooling was applied for a previous hour, night cooling is applied for the current hour, i.e. the maximum flow rate is applied. However, if the current outdoor temperature is higher than 25°C, an air flow rate is reduced to the lowest possible point (30dm^3/s).

2. Indoor and storage temperatures are calculated from a heat balance.

3. If the indoor temperature is lower than 16.7°C, which is the intended indoor temperature for bedrooms [45], night cooling is stopped.

3-4-3 Results

After hourly calculations are done, the number of hours when indoor temperature exceeds 25°C is calculated. If the number is higher than 100 hours per year, the maximum flow rate is increased and/or solar irradiation, at witch solar shading is applied, is reduced. What is more, a solar shading type can be changed. Then the simulation is run over again and the optimum air flow rate, solar shading type and irradiation value at which it turns on are determined. Figures 3-6 and 3-7 show the results when the indoor and outdoor louvers, respectively, are used as a solar shading device.

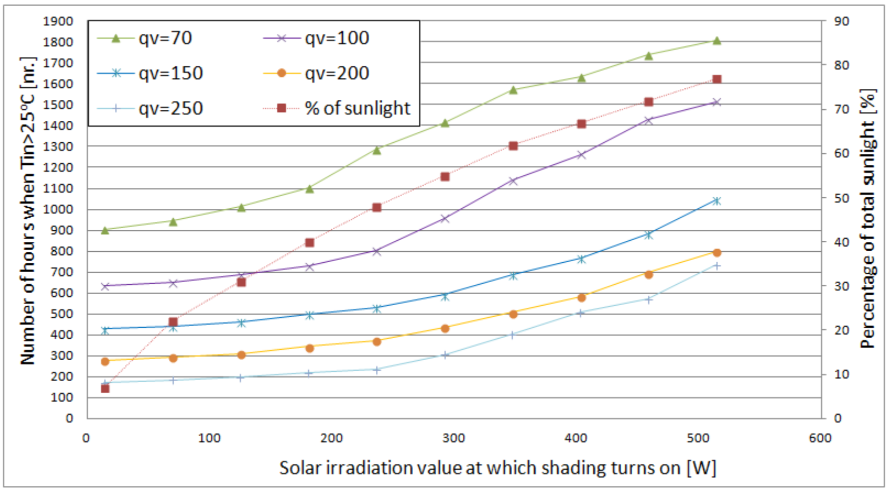

Figure 3-6: 25°C exceeding hours dependency on maximum air flow rates and solar irradiation value at which solar shading turns on. Indoor louvers are used

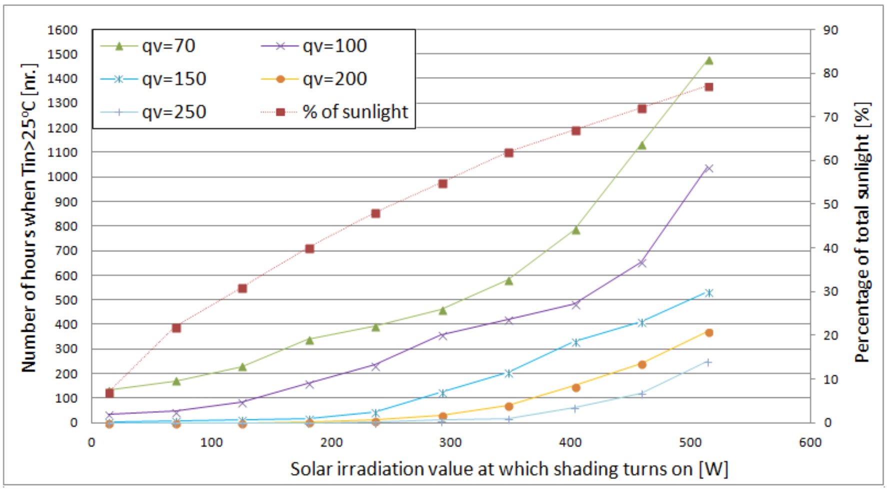

Figure 3-7: 25°C exceeding hours dependency on maximum air flow rates and solar irradiation value at which solar shading turns on. Outdoor louvers are used

It can be seen from the both figures that if the maximum air flow rate is reduced, solar shading has to switch on earlier. However, the occupants would like to enjoy morning sunshine as long as possible, so the balance should be kept between the reduced flow rate and the available hours of sunshine. Moreover, it can be seen from figure 3-6 that the number of hours when indoor temperature exceeds 25°C is higher than 100 at any flow rates. Because of this, outdoor louvers have to be used (Figure 3-7). It is chosen that at least 60% of the sunshine should be available to the house, then the maximum flow rate should be 200 dm^3/s since it represents 100 hours when indoor temperature exceeds 25°C.
Knowing the solar shading type, the irradiation value at which the solar shading turns on and the maximum air flow rate, the overall ventilation flow rates are found for three months. This is shown in figure 3-8.

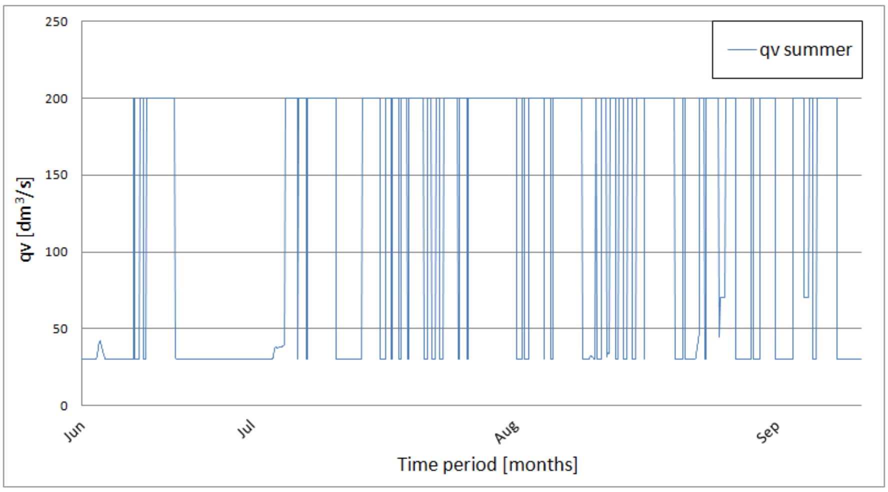

Figure 3-8: Overall air flow rate for three months at given conditions

3-5 Overall Ventilation Flow Rates

Knowing separate flow rates for carbon dioxide, humidity and excessive heat control, the total ventilation flow rate is found by merging all flow rates to the resultant flow rate. All separate air flow rates are demonstrated in figure 3-9, whereas in figure 3-10 the resultant air flow rate is shown.

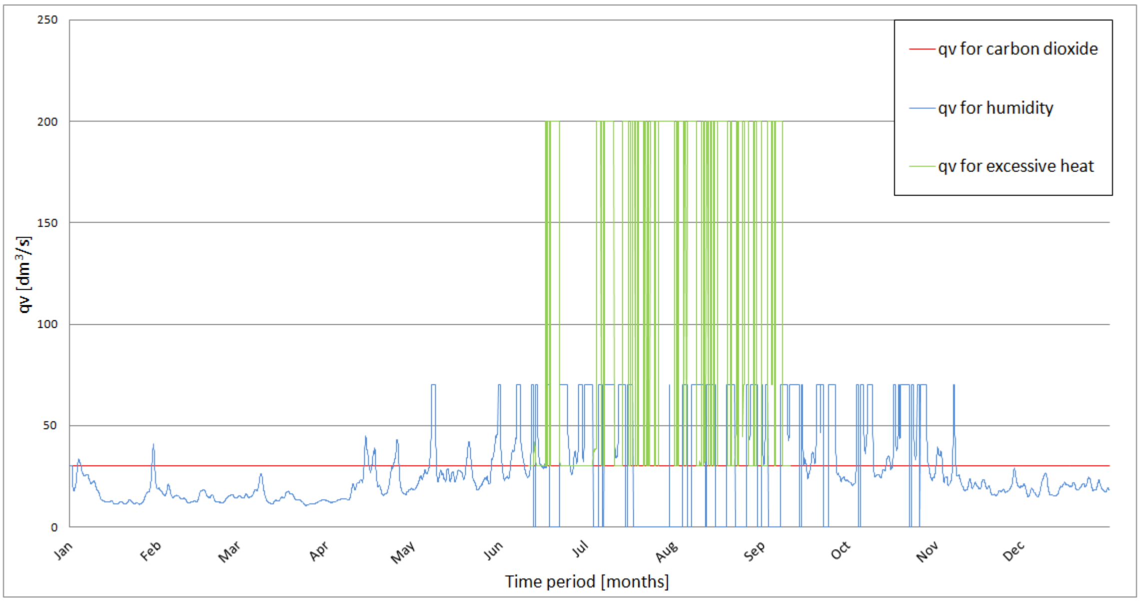

Figure 3-9: Flow rates for carbon dioxide, humidity and excessive heat control

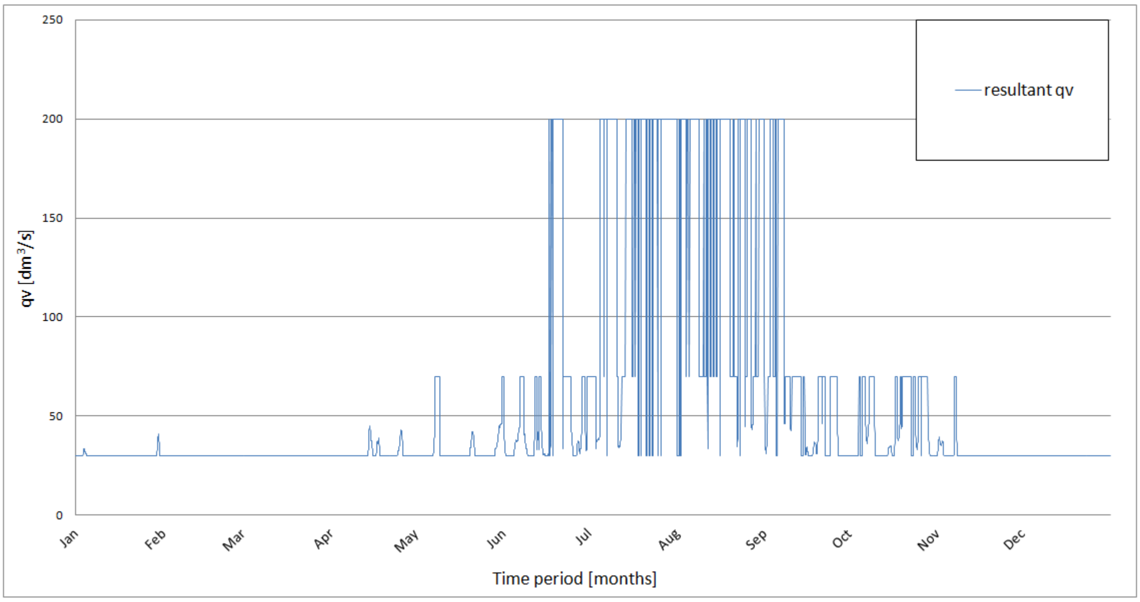

Figure 3-10: Resultant air flow rate for whole year

Chapter 4

Heat Recovery Unit

Since the required air flow rates in the cold year period are already known, the medium through which the air should flow and regain part of heat is investigated. As it has already been said, the air-to-air counter-current heat exchanger will be designed for this purpose.

In order to eliminate water clogging and reduce the density of filters, the heat exchanger consists of bigger channels than a conventional one. Although the type of the heat exchanger is already specified, a heat exchanger can have many different modifications. In order to compare separate heat exchanger models, its four characteristics, the used material and space as well as efficiency and pressure drop are compared expressing them through a monetary value. If the size of a heat exchanger is known, the material used for its production and the occupied space can be found. Pressure drop is converted into electricity consumption, knowing the air flow rate and the fan efficiency. The heat exchanger efficiency is converted into heat cost, which is regained from the exhaust air. The size of the heat exchanger is calculated using its geometry. Pressure drop and efficiency are found by using the steps presented in section 2-5. In the cold season, the outdoor temperature is lower than the indoor. Knowing the ventilation flow rate, indoor and outdoor temperatures, the heat which is lost when exchanging the warm indoor air for the cold outdoor air is calculated. Then, the lost heat is converted into the lost monetary value. The lost heat flow is calculated by using a slightly modified equation 2-14:

$$Q = c_{p,a}\rho_a q_{v,a}(T_{in} - T_{out}) \tag{4-1}$$

Here T_{in} is assumed to be always at 19.7°C due to perfectly working heating system. Then the monetary value is calculated by using the following equation:

$$Cost_{h,total} = Q * time * NG_{price} \tag{4-2}$$

In the end, the heat exchanger efficiency represents which part of the monetary value is regained.

The power which is needed for the ventilation fan is calculated by using equation 2-26. Then electricity cost is found by using the following equation:

$$Cost_{el,total} = Power * time * EL_{price} \tag{4-3}$$

The electricity and natural gas prices for end users, including taxes and levies, are taken from the *Eurostat* database [46]. A households electricity price in the Netherlands for 2013 is 0.1916 $euro/kWh$. A natural gas price is 22.56 $euro/GJ$ for the same year.
For the comparison of the different models, it is assumed that the heat exchanger is used for seven months a year. Models comparison calculations are done for 20 years in order to reduce the influence of initial material and space costs on the total costs.
Since the used material does not have almost any influence on the heat exchanger's efficiency due to its small thickness, plastic is chosen for the calculations. A plastic sheet (0.000508 m thickness) price is 6 $euro/m^2$ [47]. Nevertheless, plastic sheets have to be processed, so the initial price is multiplied by 2.5 to get the price of the processed plastics. The space cost is 400 $euro/m^3$. The both prices are taken from [48].
The amount of the material used for ventilation ductwork and the occupied space are assumed values. The material used for the ductwork is 40 m^2. The space used for the ductwork is 1.5 m^3.
According to the [8, Appendix A], at least EU4 (or G4) filters should be used for air filtration. EU4 filters have 90% of the average arrestance and 75 Pa pressure drop for the designed air flow rate of 77 dm^3/s [49, p.500].
Pressure drop through the ventilation ducts in the 'Tussenwoning' is taken from the TNO database [50], where pressure drop is calculated for the optimized ductwork. The total pressure drop through incoming and exhaust air ducts is 73.3 Pa for the design air flow rate of 77 dm^3/s. The total pressure drop at the design value is 148.3 Pa. By using equation 2-25, the constant value ($Const$) is determined (see below). Pressure drop for other flow rates is calculated by using this constant.

$$Const = \frac{dP_{design}}{{q_{v,design,a}}^2} = \frac{148.3}{0.077^2} = 25013 \tag{4-4}$$

Whereas, in the warm year period, the ventilation system switches from a balanced to exhaust-only system where both ventilation ducts are used for air exhaust. Due to pressure difference created by the exhaust system, the air is supplied through burglar free side-grills which are located in the bedrooms and the living room. The air filters are also bypassed in the warm period of the year. Therefore, the constant value for summer ($Const_{summer}$) is calculated as follows:

$$Const_{summer} = \frac{dP_{design}}{2 * {q_{v,design,a}}^2} = \frac{73.3}{2 * 0.077^2} = 6182 \tag{4-5}$$

Despite the fact that many variables are changing in different heat exchanger models, some of them remain constant. Constant factors are presented in table 4-1.

Constant	Notation	Value	Units
fan efficiency	ε_{fan}	30	%
relative roughness of heat exchanger channels	ω	$5 * 10^{-6}$	–
electricity price	El_{price}	0.1916	$\frac{euro}{kWh}$
natural gas price	NG_{price}	22.18	$\frac{euro}{GJ}$
processed plastic price	Pl_{price}	15	$\frac{euro}{m^2}$
space price	Sp_{price}	400	$\frac{euro}{m^3}$
material used for ducts	Mat_{duct}	40	m^2
space used for ducts	Sp_{duct}	1.5	m^3
dynamic viscosity of air	η_a	$1.82 * 10^{-5}$	Pa, s
thermal conductivity of plastic	λ_{pl}	0.21	$\frac{W}{mK}$

Table 4-1: Constants used in calculations

4-1 Four Heat Exchanger Models

A heat exchanger can be designed in many different ways. Nevertheless, after a meeting with industrial designers, the four most promising models are decided to investigate and compare under equal conditions. In this section, all the four models are presented and the main implied advantages and disadvantages of every of them are discussed. Figures of the models show the cross-sectional area of the heat exchanger's concept. For the sake of simplicity, it is assumed that the diameter and the height of the heat exchangers are of the same size since it does not influence final results. However, in reality, they can be adjusted to different circumstances. A figure of every model presents how the height of a channel is understood ($H_{element}$ in the figures). This is important for further calculations. If a model has movable parts, a figure shows several positions of the model. Green arrows show which points are moved while folding and to which directions. Folding enables air to bypass a heat exchanger with low pressure drop when the heat exchanger is not necessary and higher air flow rates are needed, e.g. in the warm season. The outgoing air flow is noted with a 'plus' and the incoming air flow with a 'minus'. Every heat exchanger's model consists of small channels. Each side of the channels faces two flows: on the one side, an outgoing flow and on the other side, an incoming flow. Hence, the heat exchanger's area is used in the most productive way.

4-1-1 MODEL-1

Model-1 consists of squared channels which allow the heat exchanger's folding, as it is shown in figure 4-1 (positions 2 and 3). This model is least rigid since not only inside walls are flexible but also the whole outer frame changes its size while folding.

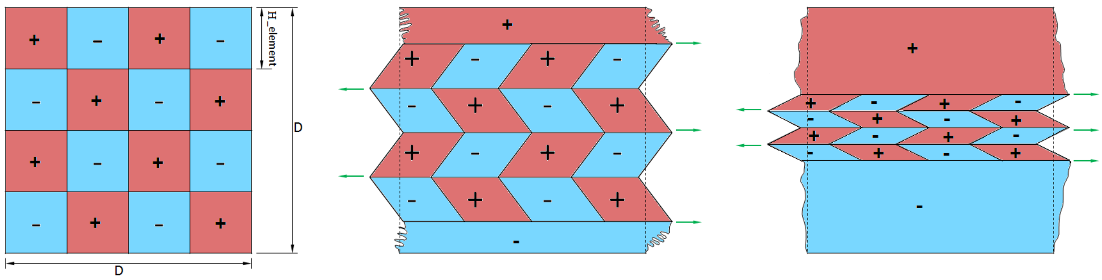

Figure 4-1: MODEL-1. Position 1: heat exchanger in use. Position 2: intermediate step. Position 3: bypassing ducts in use

4-1-2 MODEL-2

Model-2 consists of long rectangular channels. As in Model-1, the rectangular channels allow the heat exchanger's folding, as it is shown in figure 4-2 (positions 2 and 3). Model-2 does not cross outer duct walls, so it is more rigid than Model-1. Due to its geometry, it also makes easier to separate incoming and outgoing flows at the end of the heat exchanger. Yet, it has less heat exchanging surface than Model-1 and consequently, lower efficiency.

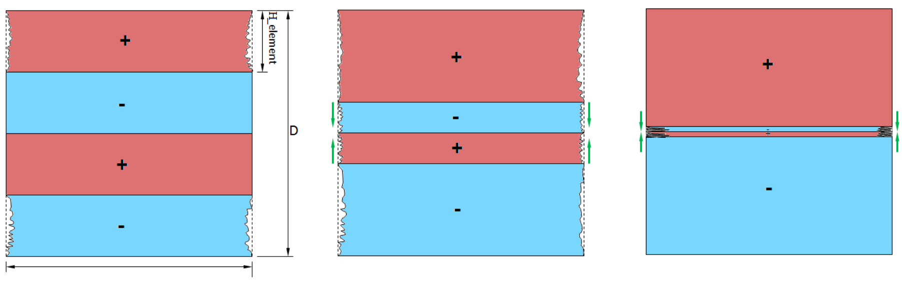

Figure 4-2: MODEL-2. Position 1: heat exchanger in use. Position 2: intermediate step. Position 3: bypassing ducts in use

4-1-3 MODEL-3

Model-3 consists of the equilateral triangle channels. When the heat exchanger is not necessary and higher air flow rates are needed, the triangle channels are squeezed towards each other. Due to its flexible side walls, the triangles change its geometry eventually becoming rectangular. While squeezing, outgoing flows in one half and incoming flows in the other half are blocked. In the end, half of the duct contains only the incoming flows, the other half only the outgoing flows. Model-3 is shown in Figure 4-3. Model-3, as well as Model-2, does not cross outer duct walls. Furthermore, as it can be seen at first glance, Model-3 has a larger heat exchange area than Model-2 and Model-1. However, when the channels are squeezed, part of the flow still have to go through the rectangular (in position 3), thus having a small cross-sectional area. As a result, it can cause high pressure drop when flow rates are enlarged.

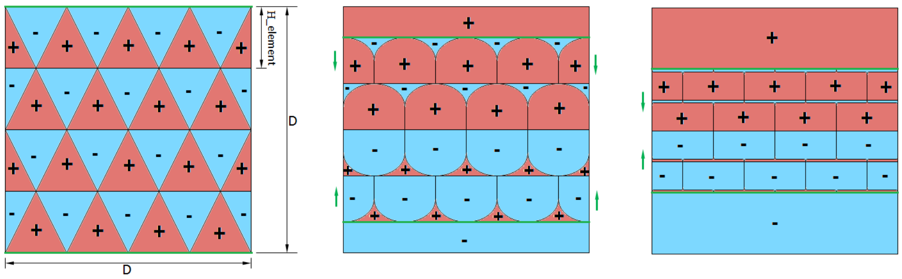

Figure 4-3: MODEL-3. Position 1: heat exchanger in use. Position 2: intermediate step. Position 3: partly bypassing ducts in use

4-1-4 MODEL-4

Model-4 has a very similar construction to that of Model-3. In addition to triangle channels, it also has two bypassing ducts. When the heat exchanger is not necessary and higher air flow rates are needed, the flows are directed to bypassing ducts by external valves. Model-4 is shown in figure 4-4.

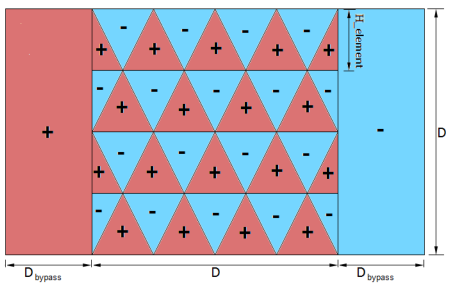

Figure 4-4: MODEL-4

The advantages of the first three heat exchangers with a folding mechanism are: the saved space, by accommodating two units into one, and the possibility to use only part of the heat exchanger (position 2 in the figures). The disadvantages are: the systems, due to flexible walls, are less rigid and extra machinery for folding is needed. Model-4, however, has no movable parts and so is very rigid, but the bypassing ducts take extra space and material. A simple comparison of all the four models, based on the estimated advantages and disadvantages, is shown in table 4-2. Note that the comparison is meant only to compare the models with one another, so it does not present any quantitative information.

Issue	Model-1	Model-2	Model-3	Model-4
construction complexity	high	low	high	high
folding complexity	very high	high	very high	-
level of required machinery	high	high	high	low
required space	medium	low	low	high
heat exchange surface area	high	low	very high	very high
pressure drop in winter	high	low	very high	very high
pressure drop in summer	low	low	high	low

Table 4-2: Comparison of four models

4-2 Heat Exchanger's Selection

All the four models are compared under the same dimensional conditions (length, diameter and the height of elements). Table 4-3 presents the obtained results, when a flow rate in the heating and cooling seasons are 70 and 200 dm^3/s respectively. It is obvious that in reality the system does not run on 70 dm^3/s all the time, therefore, it should be noted that the presented numbers can only be used for the comparison of the different models. Prices are calculated for twenty years of operation. The comparison, with a volumetric air flow rate of 30 dm^3/s in the heating season and 200 dm^3/s in the cooling season, are given in appendix C.

qv=70 (dm^3/s)					
		MODEL_1	MODEL_2	MODEL_3	MODEL_4
Cost (€):	**TOTAL**	**7512**	**9468**	**6949**	**6727**
	electricity_winter	831	740	993	993
	electricity_summer	1382	1380	1665	1404
	lost heat	3802	5973	2703	2703
	material	861	739	951	966
	space	636	636	636	660
Dimensions (m):	L	1	1	1	1
	D	0.3	0.3	0.3	0.3
	H_elements	0.01	0.01	0.01	0.01
Parameters:	dP_winter (Pa)	143	128	172	172
	dP_summer(Pa)	127	126	178	131
	Efficiency (%)	64	44	75	75
	HE_cross-section(m2)	0.0392	0.0419	0.0375	0.0375
	heat_exchange_area(m2)	15.1	8.1	21.6	21.6

Table 4-3: Comparison of four models, qv=70 dm^3/s in the heating season and qv=200 dm^3/s in the cooling season

As it is seen from table 4-3, Models 3 and 4 have the lowest total price. The most influencing factor for these two models is a much lower 'lost heat' cost in comparison to the other two models. It means that due to high efficiency Models 3 and 4 regain more

heat, so the 'lost heat' cost is reduced. Obviously, efficiency is proportional to the heat exchange area, which is higher for these two models. Consequently, two conclusions can be drawn from this comparison: 1) triangle geometry channels have the highest heat exchange area; 2) the heat exchanger's efficiency is the most important factor for the heat exchanger's design if flow rates are high enough.
Yet, it is seen that Model-3 has a higher electricity cost in summer than Model-4. The reason behind is seen in figure 4-3, position 3. When Model-3 is squeezed, part of the air can freely move through a rectangular opening. Yet, another part of the air has to go through the channels of smaller hydraulic diameters, which increases pressure drop. Although it is partly compensated by a lower space and material cost, low pressure drop in Model-4 has a higher influence on the total price. Having summed up all the results, Model-4 is chosen for further investigation.

4-3 Optimization of Model-4

After the comparison of the models, Model-4 is selected as the most promising one. Still, it has to be optimized. Optimization is done by changing the heat exchanger's length, diameter, height of elements and the size of bypassing ducts. A new program is written for this purpose. The program applies to different sets of dimensions. All dimensions are allowed to be freely changed. Only the height of the heat exchanger's channels is constrained. In order to avoid water blockage, the channels are not allowed to be smaller than 0.005 m. Then, the program calculates the total cost for every set and compares the prices. In the end, it selects the best set of dimensions, based on the lowest total cost. A preliminary initial cost of the system, including material and space costs, is also determined.

The total cost depends on an air flow rate as well. The use of dynamic air flow rates, which are found in Chapter 3, would demand a lot of computer resources, so the most suited constant air flow rate is determined. It is assumed that the heat exchanger is needed for 7 months a year (from October 1st till May 1st). Then the needed flow rates of these months are sorted from the smallest up to the largest. Flow rates are taken from Chapter 3. The results are shown in figure 4-5.

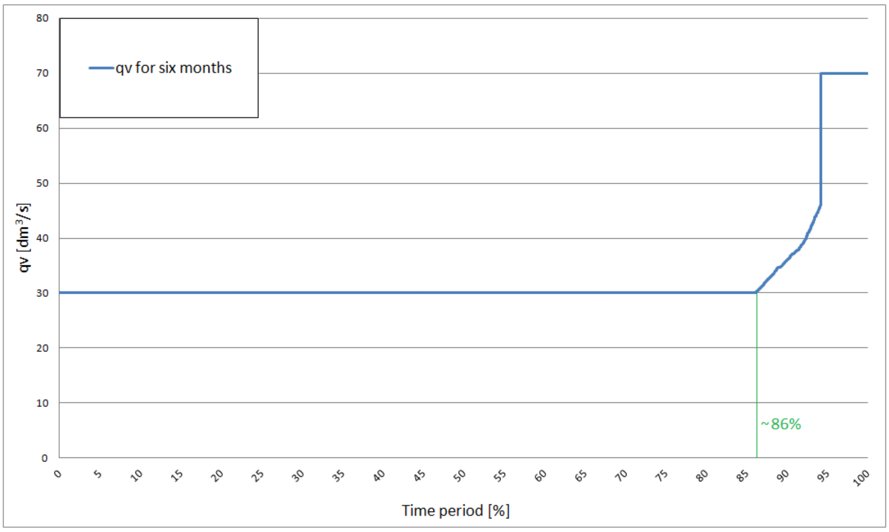

Figure 4-5: Sorted flow rates for seven months of the heating season

From figure 4-5, it is seen that more than 85% of all the time the required flow rate is 30 dm^3/s. Hence, this flow rate is used for the heat exchanger's optimization. The results are presented in table 4-4.

Optimized characteristic	**Notation**	**Value**	**Units**
heat exchanger's length	L	0.7	m
heat exchanger's diameter	D	0.25	m
elements height	$H_{elements}$	0.005	m
bypassing duct diameter	D_{bypass}	0.1	m
preliminary cost of the system	$Cost$	1562	€

Table 4-4: Optimized heat exchanger's characteristics

4-4 Yearly Energy Consumption Calculation

In order to calculated yearly energy consumption, the program used for the comparison of the models is modified and adjusted to dynamic air flow rates. It is assumed that the heat exchanger is used for seven months, so the ventilation system switches to exhaust-only mode for the other five months. It is assumed that the heating system ensures an indoor temperature of 19.7°C at any time of the heating season (seven months). However, if outdoor air temperature is higher than 17.7 °C, indoor air temperature follows equation 3-2. The optimized heat exchanger model is used for this period. Pressure difference due to the stack effect is also calculated and subtracted or added (depending on a sign) from ductwork and heat exchanger pressure drop. Figure 4-6 depicts pressure drops and volumetric air flow rates of the whole year.

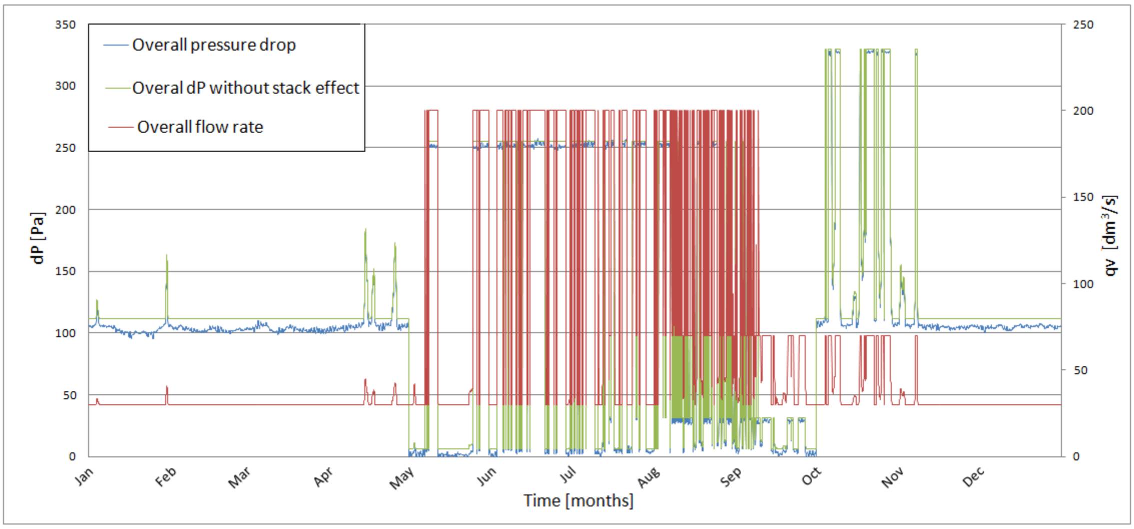

Figure 4-6: Pressure drops and air flow rates for whole year

A switch from a balanced to exhaust-only ventilation system is clearly seen. Although air flow rates are almost tripled in some periods of the cooling season (see the July-September period), the maximum pressure drop is lower than 260 Pa, whereas the maximum pressure drop of 70 dm^3/s in the heating season is around 330 Pa. It is seen that the stack effect contribution to the reduction of pressure drop in the heating season is much higher than in the cooling season (blue line), yet, in general, it remains very low. Lost heat with and without the heat exchanger is shown in figure 4-7.

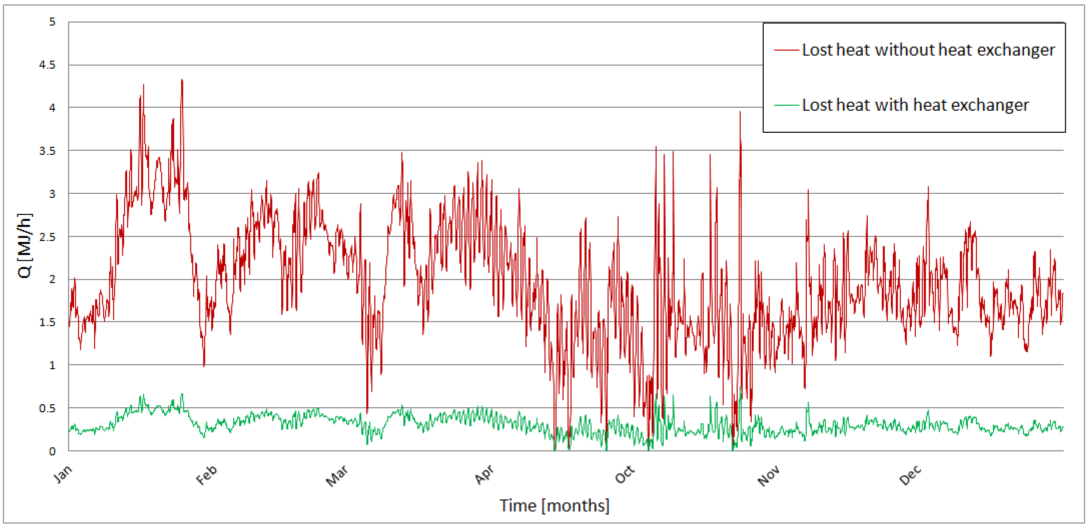

Figure 4-7: Lost heat with and without heat exchanger

Knowing the lost and regained heat as well as the pressure drop of the system at every hour of the year, the total amount of electricity and lost heat as well as the costs for the whole year are calculated. The results are given in table 4-5.

Issue	Value	Units
electricity consumption in winter	75.1	kWh
electricity consumption in summer	260.2	kWh
total electricity consumption	335.3	kWh
total electricity cost	64.2	€
lost heat through ventilation (winter)	9.97	GJ
regained heat using heat exchanger	8.4	GJ
regained heat using heat exchanger	84.4	%
lost heat using heat exchanger	1.6	GJ
lost heat cost using heat exchanger	34.5	€
total yearly energy cost (with heat exchanger)	98.8	€

Table 4-5: Year round energy cost calculation

Chapter 5

Experiment

In section 2-5-2, it is mentioned that the heat transfer coefficient from the air to the wall or from the wall to the air are very important. Although there are several theoretical and empirical equations describing the mentioned coefficient, their results are quite distinct. Empirically determined equation 2-17 is used for this research, but it is not clear whether this equation reflects the real heat transfer coefficient values. As a result, experiments are carried out to determine the real value of the coefficient.

5-1 Experiment Setup

In order to calculate the heat transfer coefficient value, two, counter-current heat exchangers are made. Since the material of the heat exchanger is of no importance, they are made out of cardboard. Cardboard is chosen because it is easy to work with. In figures 5-1, 5-2 and 5-3, the production sequence is shown.

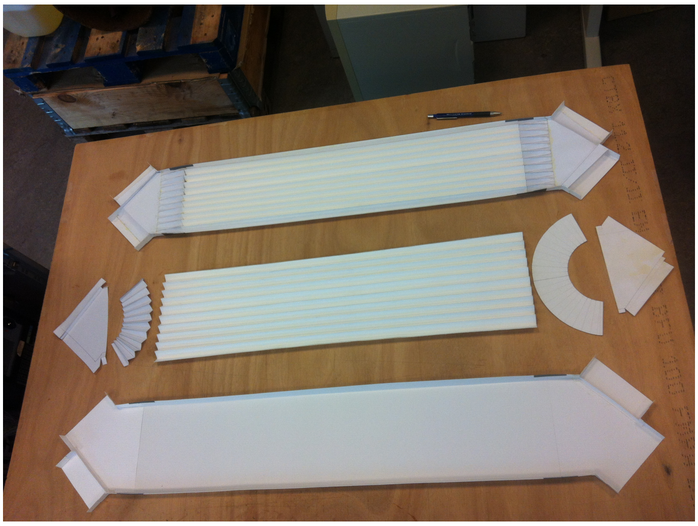

Figure 5-1: Production of separate layers

Separate layers are produced. Firstly, the casing of the layer is made with a separation of the flows (figure 5-1, at the bottom). Then a harmonica-type heat exchanging surface is made with a transition from the harmonica to flat surface part (the middle part of the figure). At the end, the harmonica type and the transition parts are glued together and placed in the casing (the upper part of the figure).
In figure 5-2, the heat exchanger's all separate layers are shown.

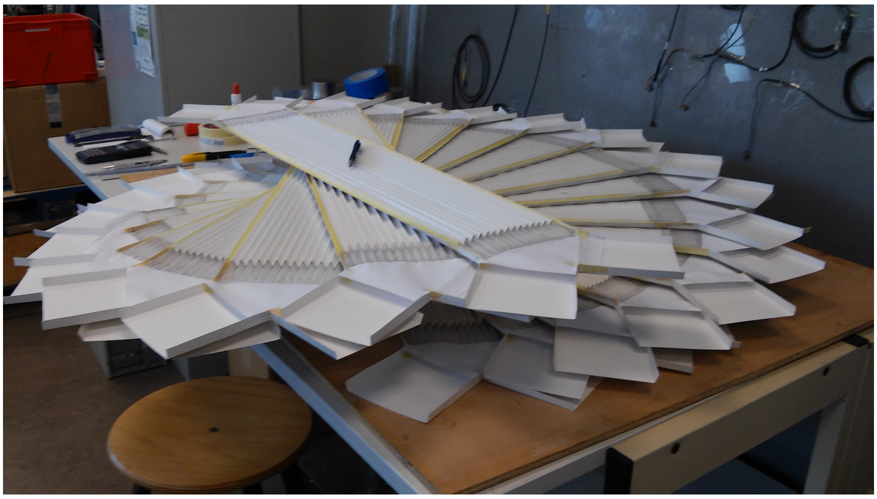

Figure 5-2: Separate heat exchanger's layers

Figure 5-3 shows all the parts glued on top of one another to make two main parts of the heat exchanger. These two parts are glued together after placing thermocouples for the temperature measurements. All cracks are taped with special duct-tape to avoid air leakages.

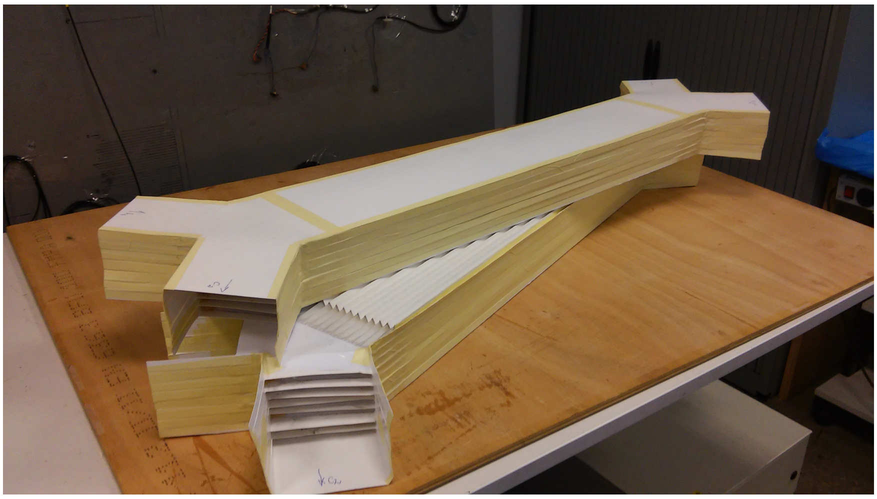

Figure 5-3: Two parts of heat exchanger

The main difference between the two heat exchangers is the size of heat exchanging channels. Since the shells of the heat exchangers are of the same size, the heat exchanging surface area is also higher in the second model. The main characteristics of the both models are given in table 5-1.

	Heat exchanger 1	**Heat exchanger 2**
length (m)	0.72	0.72
diameter and height (m)	0.15	0.15
thickness of the wall (m)	0.0005	0.0005
thermal conductivity ($\frac{W}{mK}$)	0.21	0.21
height of the channels (m)	0.013	0.00866
total surface area (m^2)	3.132	4.752
cross-sectional area (m^2)	0.00975	0.00974

Table 5-1: Characteristics of two heat exchanger models

After the heat exchangers are done, thermometers are attached to its all four outlets and inlets. In addition to that, ten thermocouples are placed between the two parts to measure the temperature in separate parts of the heat exchanger. Diameter-wise: five thermocouples are put in the center, other five a side, throughout the length of the heat exchangers. Height-wise: all the thermocouples are located in the middle of the heat exchangers. The places of the thermocouples are shown in figure 5-4.

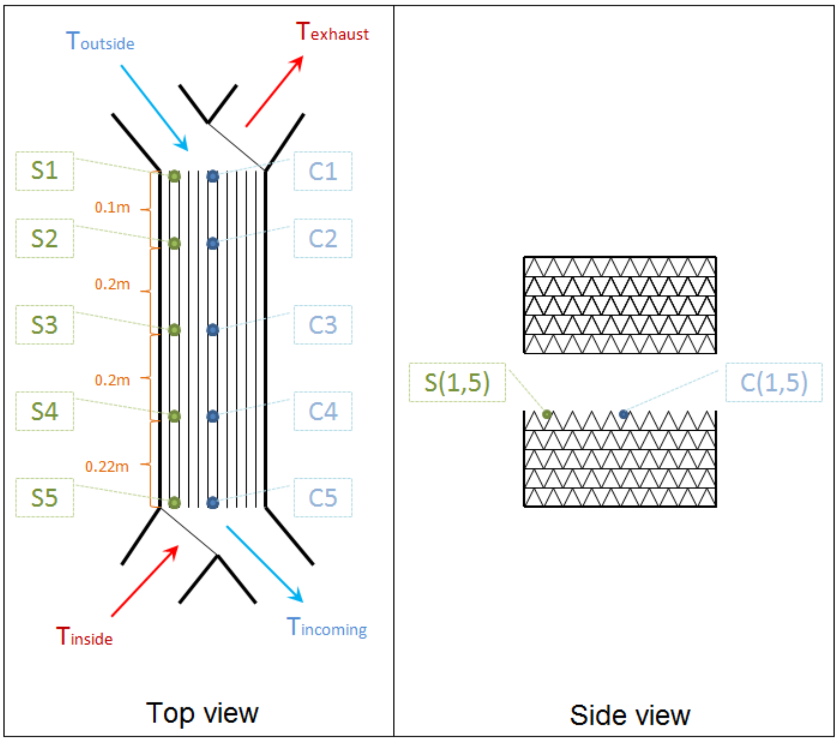

Figure 5-4: Placement of thermocouples; S-side, C-center

Then the heat exchangers are insulated and placed in a climate chamber under two different conditions. Every heat exchanger is also tested with three separate flow rates. Consequently, in total, there are six different setups for each heat exchanger. More pictures of the experiment are presented in appendix E. All six test conditions are presented in table 5-2.

Test No.	**Outdoor temperature (C)**	**Outdoor relative humidity (%)**	**Indoor temperature (C)**	**Indoor relative humidity (%)**	**Air flow rate (m^3/s)**
1	5	70	25	28	0.034
2	5	70	25	28	0.024
3	5	70	25	28	0.014
4	−5	70	20	15	0.034
5	−5	70	20	15	0.024
6	−5	70	20	15	0.014

Table 5-2: Test conditions

Since cardboard is sensitive to water, the *MollierSketcher* software [51] is used to confirm that there will be no water condensation during the experiment.

5-2 Experimental Results

The time span for every test condition is one hour. Measurement data are written in a file every twenty seconds. When all six tests for both heat exchangers are done, average hourly values are calculated and analyzed. The efficiency values are computed for both outgoing and incoming flow rates. Then the average measured efficiency is found and compared with the theoretically calculated values. A comparison is shown in figure 5-5.

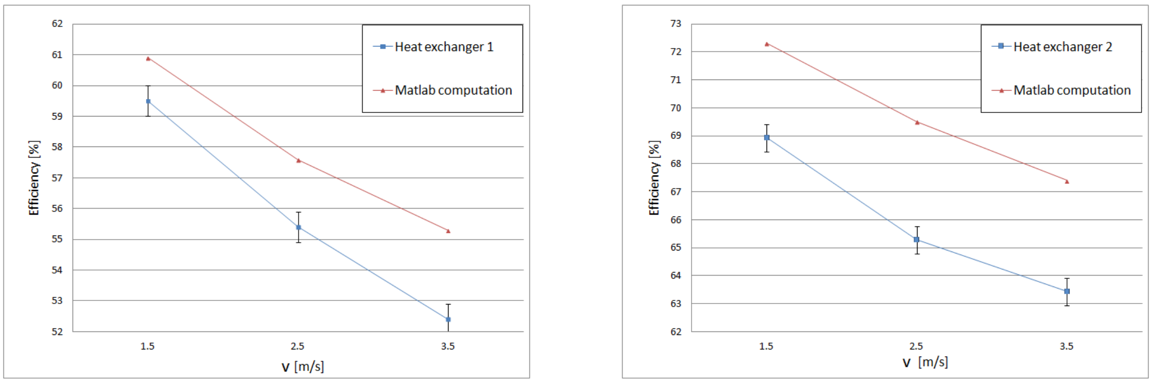

Figure 5-5: Computed and measured efficiencies

As it is seen, the computed efficiencies match the measured ones very well. The biggest difference for heat exchanger 1 is only 2.9% (at 3.5 m/s) (if accuracy bars are disregarded), whereas it is 4.2% for the second heat exchanger (at 2.5 m/s).
The heat transfer coefficient values are calculated by using a reverse sequence of the steps which are mentioned in section 2-5-1. Resultant graphs where the theoretically and experimentally determined heat transfer coefficient values are compared are shown in figure 5-6.

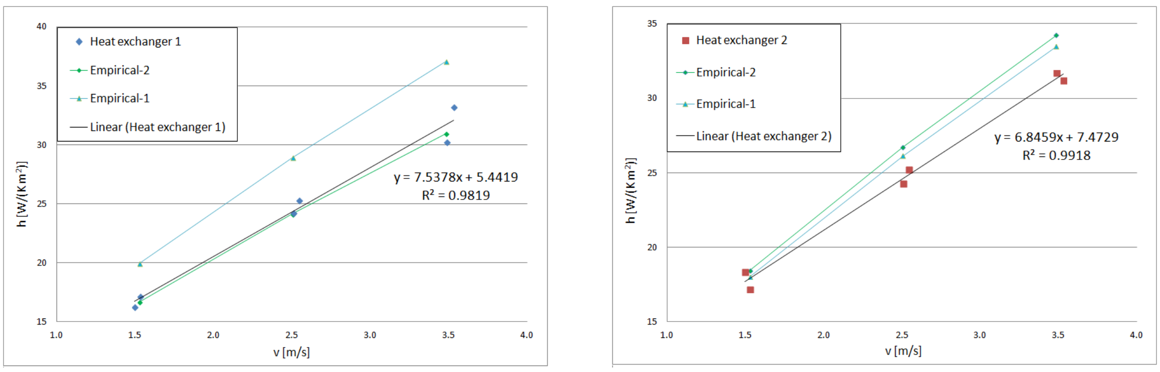

Figure 5-6: Empirical and measured heat transfer coefficient values

It is seen that the measured (and then calculated) heat transfer coefficient values of heat exchanger 1 almost perfectly match '$empirically - 2$' values, whereas, '$empirically - 1$' values differ slightly more. The measured heat transfer coefficient values of the second heat exchanger are very similar to the two empirically determined curves' values. In this case, the '$empirical - 1$' values are closer than '$empirical - 2$' to the measured ones, although the difference is very little. A conclusion can be drawn that the both '$empirical - 1$' and '$empirical - 2$' values are close approximations of the real results. Still, the heat transfer coefficient depends on the heat exchanger's channels height, therefore, '$empirical - 1$' presents a better approximation of the real values if $h_{element} = 0.01m$, whereas '$empirical - 2$' is more accurate when the height of the elements is $0.015m$.

The results obtained from the thermocouples are presented in figure 5-7.

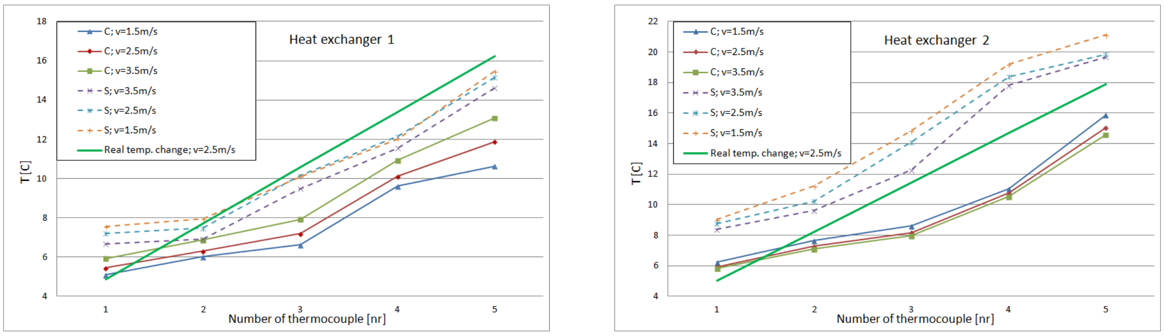

Figure 5-7: Thermocouples' measurements (thermocouple error 0.5 K, temperature sensors absolute accuracy 0.07 K)

As it is expected, the thermocouples show a gradually increasing temperature throughout the heat exchangers length. However, it is seen that side-located thermocouples show higher temperatures than center-located. Moreover, a real temperature change, which is measured by using the thermometers positioned at the end of the heat exchanger, does not match the start and end positions of the thermocouples (Note: a temperature change path can be different but the end point temperatures should match). The most probable reason for this is the fact that the heat exchanger was not provided with air flow distributing borders, so an air flow rate is not equally distributed throughout the heat exchanger's cross-sectional area. As a result, since the thermocouples measure temperature only at one channel of the heat exchanger, it is possible that the flow rate is faster or slower at that particular channel than at the rest of the channels. Consequently, it is possible that the measured end temperature is higher in the side channels than the total temperature of the heat exchanger.
As it was expected, the pressure drops of both models are very high. This is because the heat exchangers are made manually, without taking care of pressure drop reduction. Nevertheless, pressure drop measurement is not intended to be a purpose of this experiment.

Chapter 6

Year Round Energy Consumption Calculation Using Wind Cowl

As it is seen from table 4-5, whole year electricity consumption is moderate. Nevertheless, in this chapter, it is investigated what part of total yearly electricity consumption can be saved with the help of renewable energy, e.g. a wind cowl.
Based on the example house size (see 3-1), the estimated wind cowl position is on the rooftop, 11 meters above the ground. Then, by using wind data and equation 2-28, an hourly wind speed at the cowl's level is computed.
Fourteen rotating and stationary wind cowls and openings are investigated. Experimentally determined characteristics of all the wind cowls and openings are presented in appendix D. It is assumed that a wind flow is perpendicular to the cowls' position since the exact vertical angle at which the wind approaches the cowls, according to [34], has only a minor influence on final results. The cowl '*number 12*' is selected for further research because it has the highest overall pressure coefficient at a zero degree angle. The cowl '*number 12*' is shown in figure 6-1.

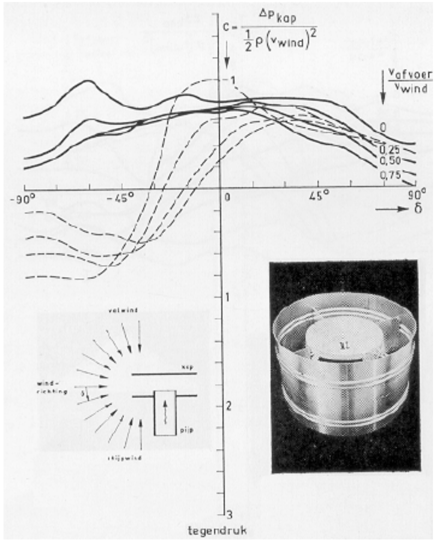

Figure 6-1: Selected wind cowl characteristics

Since research [33] compared the tube opening (see '*Wind cowls: Nr. 1*' in appendix D) with other cowl types, the dotted lines represent open tube pressure coefficients. The dotted lines are disregarded. By taking into account the shape of the cowl, it is assumed that the friction coefficient of cowl is 0.3 [28, 83p.]. The pressure coefficient is the function of air velocity in the outgoing duct and a wind speed ratio. The wind speed is taken form the measured data, while the air velocity in the duct is calculated by dividing the air flow rate by the duct's cross-sectional area. Using the speed ratio and figure 6-1, the pressure coefficient dependence on the wind and the air in the duct speed ratio is presented in equation 6-1.

$$C_{pressure} = -0.132\frac{v_{duct}}{v_{wind}} + 0.8 \tag{6-1}$$

When $0 < v_{duct}/v_{wind} < 1$.
Studies [32] and [33] investigated only a natural ventilation ($v_{duct} < v_{wind}$). However, in a hybrid ventilation, v_{duct} can be much higher, especially in summer, than v_{wind}. Since pressure drop coefficient values are not known when the wind speed is lower than air velocity in a duct, two cases are distinguished:

1. The equation above is used until air velocity in a duct gets higher than the wind speed. Above that the pressure coefficient value is zero. In this case, it is assumed that the cowl does not assist the ventilation fan at all on the mentioned condition.

2. If air velocity in a duct is higher than the wind speed, the pressure coefficient value is still gradually decreasing, following the curve which is determined by using the known values. In this case, it is assumed that even with a wind speed lower than the air velocity in the duct, the cowl assists the ventilation fan. However, when the ratio between the two speeds is increasing, the pressure coefficient is reducing.

The both cases representing pressure coefficient lines are shown in figure 6-2.

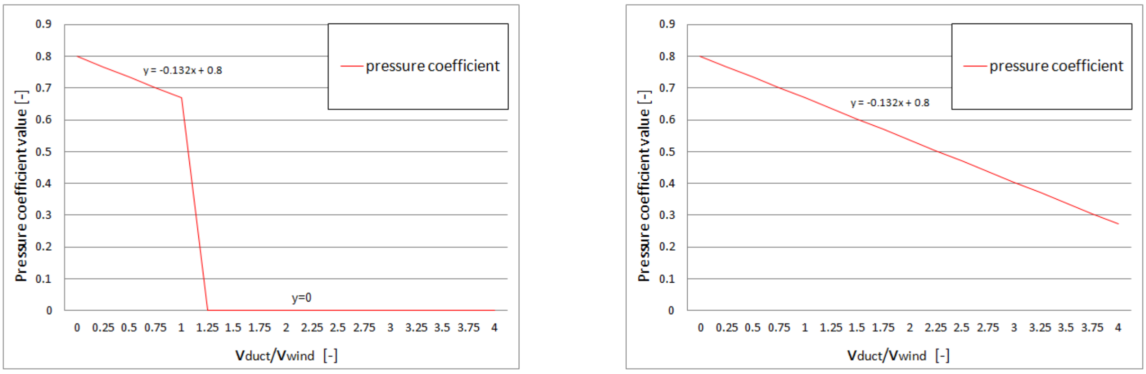

Figure 6-2: Pressure coefficient cases. Case nr. 1 (left), case nr. 2 (right)

Case 1 might be underestimated since it is quite obvious that even if the wind speed is lower than air velocity in a duct, it still should ease an air flow through the duct at a certain degree. On the other hand, case 2 might be overestimated since it assumes that, for example, even if air velocity in a duct is three times higher (see figure 6-2, case No. 2) the pressure coefficient still has a value of 0.4. Therefore, it is expected that the real pressure coefficient values are between the two cases.
The pressure drop of the system is calculated by using a wind cowl. It should be noted that a wind cowl is placed only on the exhaust duct, so the pressure drop of the supply duct does not change. Only exhaust duct pressure drop can decrease or increase, depending on the wind speed and the air flow rate in the duct. Figure 6-3 depicts the first case ductwork pressure drop with and without a wind cowl.

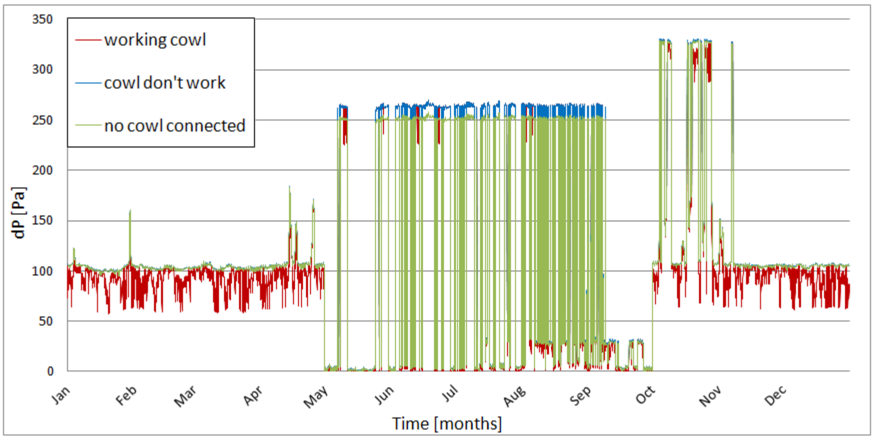

Figure 6-3: Pressure drop with and without wind cowl

It is mentioned in theory that the placement of a wind cowl already induces extra resistance since the cowl blocks the outgoing air. Pressure drop when the cowl is not connected is denoted with a *green* line in figure 6-3. Naturally, the pressure drop, due to the cowl, enhances, increasing an air flow rate (the summer part in the graph). In conclusion, wind cowls are more helpful when air flow rates in ductwork are lower. The pressure drop graph of the second case does not differ from the first case very much, so it is not shown. Table 6-1 presents year round energy calculation results by using a wind cowl.

Case 1	**Value**	**Units**
electricity consumption in winter	68.7	kWh
electricity consumption in summer	270.5	kWh
total yearly electricity consumption	339.2	kWh
total yearly electricity cost	65.0	€
Case 2	**Value**	**Units**
electricity consumption in winter	68.7	kWh
electricity consumption in summer	265.1	kWh
total yearly electricity consumption	333.7	kWh
total yearly electricity cost	64.0	€
Both cases	**Value**	**Units**
lost heat through ventilation (winter)	9.97	GJ
regained heat using heat exchanger	8.4	GJ
regained heat using heat exchanger	84.4	%
lost heat using heat exchanger	1.6	GJ
lost heat cost using heat exchanger	34.6	€
total yearly energy cost case 1 (with heat exchanger)	99.6	€
total yearly energy cost case 2 (with heat exchanger)	98.6	€

Table 6-1: Yearly energy consumption

It is seen, from table 6-1, that although case 2 has lower electricity consumption in summer, the both cases have very similar results. It can be concluded that the both cases can be chosen for the approximation of pressure coefficient values when air velocity in a duct is higher than the wind speed. The first case is selected for further calculations. A wind cowl influence on yearly electricity consumption is shown in table 6-2.

Issue	Value	Units
electricity which is saved using cowl in winter	6.4	kWh
electricity which is saved using cowl in winter	8.5	%
electricity which is saved using cowl in summer	-10.3	kWh
electricity which is saved using cowl in summer	-3.9	%
total electricity which is saved using cowl	-3.9	kWh
total electricity which is saved using cowl	-1.2	%
total electricity cost which is saved using cowl	-0.8	€

Table 6-2: Yearly electricity consumption with and without wind cowl

It is seen that savings in winter reach 6.4 kWh, whereas summer savings, due to high air flow rates, get a negative value. The total electricity consumption gets a negative value when using a wind cowl. It should also be noted that the cowl's and its placement prices are not included into the calculations. Study [34] has found a 25% reduction in yearly electricity consumption when using a wind cowl, however, in the mentioned study the air flow rate was lower (55 dm^3/s) and the pressure drop included only a straight duct.

Chapter 7

Discussion

In this chapter, a very brief research description is presented in order to familiarize the reader with the source from which the upcoming conclusions are drawn. It also provides a short description of the new system and its functionality.

A ventilation system is improved by using the best parts of already existing ventilation systems. A newly developed system operates on a heat recovery unit in the heating season to regain heat which otherwise would be exhausted to the surrounding environment. Air flow rates are well controlled and can be directed to the desired indoor areas. In the warm season, bypassing ducts are employed, allowing us to have higher air flow rates with a lower pressure drop. Apart from that, the ventilation switched from balances to exhaust-only system, where both passages are used for the exhaustion of the indoor air, reducing the pressure drop even further. The fresh outdoor air enters the dwelling through burglar-free grids which are located in the bedrooms and the living room, the rooms where fresh air is needed most. Such a configuration allows us to provide the dwelling with fresh air and natural cooling on demand. At the same time, the ventilation system's efficiency is considerably enhanced because energy is saved in heating and cooling seasons.

In the cold year period, the developed system employs a modified air-to-air countercurrent heat exchanger. The exchanger accommodates larger heat exchange channels compared to conventional systems. Bigger channels have several important advantages: They prevent condensed water blockage and freezing, reduce pressure drop, ease the cleaning of the unit, require lower density filters. On the other hand, due to larger channels, the heat exchanger efficiency is reduced. Therefore, the size of the unit has to be increased. Changing the dimensions of the unit (diameter, height, length, the size of channels, the diameter of bypassing ducts), the optimum between efficiency, pressure drop, space and material cost of a new-size heat exchanger is found.

Due to a high variation between the calculated heat transfer coefficient values by using theoretical and empirical equations, two heat exchanger models are produced and tested. The main difference between them is the size of heat exchanging channels.

The two models are tested under six different conditions. The results show that the experimentally determined data almost perfectly matched the empirically calculated values.

A renewable energy source is investigated in this research. Several wind cowls are analyzed and a selection of the cowl of the best characteristics is made. Since wind cowl usefulness is not examined when air velocity in a ventilation duct is higher than the wind speed, two boundary cases are researched. The first case states that as soon as the wind speed is lower than air velocity in a duct, the wind cowl does not contribute to ventilation. The second case, however, states that the cowl still contributes to the process, although the contribution is reduced under the same conditions. The results show that the outcome of the two cases is very similar, hence, one case is selected for further calculations. However, a conclusion is drawn that cowl contribution to ventilation due to a high duct pressure drop is very low. Therefore, it is recommended to design a low pressure distribution system before using a wind cowl.

After the investigation of the four separate models, it is found that a triangle is the most efficient geometry for a heat exchanger. This is the case because the fixed size heat exchanger, which consists of triangle channels, accommodates the largest surface area.

Optimal heat exchanger's dimensions, by using four variables, namely pressure drop, efficiency, material and space cost, are calculated, assuming that it will be used in the dwelling. However, by changing one of the variables if, for example, the used space is of minor concern, the dimensions of the system could be recalculated and the new optimum would be found. Therefore, due to a flexible way of calculating, the optimal heat exchanger's dimensions can be adjusted to different applications.

Due to a larger channel size, condensed water drains down the duct. Because of this, the heat exchanger is perfectly suitable for other high-humidity environments, such as greenhouses.

Chapter 8

Conclusions

In this chapter, the main conclusions from separate chapters are presented.

Air Flow Rates Required for New System

1. The new ventilation system provides the dwelling with a 'good' indoor air quality at any time of the year. It also ensures that thermal comfort of the dwelling is present at most times of the year.

2. Two systems, namely hight-volume exhaust-only and balanced with heat recovery, are coupled together. By doing so, night cooling in warm and the heat recovery unit in cold seasons are exercised. This allows us to save heating energy in cold and cooling energy in warm seasons, increasing the overall energy performance of the ventilation system.

3. By using minute simulations and a certain control scheme, the demanded yearly air flow rates for carbon dioxide, humidity and excess heat control are found. Typical values are 30, 70, 200 dm^3/s respectively.

4. Since the exhaust-only mode employs both supply and exhaust ducts for exhaust purposes, air outflow is very well distributed through the rooms while using the exhaust unit.

5. In warm season, solar shading is necessary to reduce incoming heat.

6. A weather forecast is used for night cooling control.

Heat Recovery Unit

1. The heat exchanger, having triangle heat exchanging channels and two bypassing ducts, shows the best performance (see figure 4-4). This heat exchanger is chosen for further calculations. Different heat exchangers are compared by using the Matlab program, which evaluates the heat exchanger's four separate parameters and represents them by one number, i.e. the total price.
2. The optimal heat exchanger specifications are found: Length=0.7 m; Diameter and height=0.25 m; channels height=0.005 m; Bypassing duct diameter=0.1 m; Preliminary cost=1562 €. Optimization is done by using the Matlab program, which compares different sets of dimensions (height, diameter, length, heat exchanging channels size, bypassing duct size) and selects the best match. The criterion for selection is the lowest total price.
3. The heat exchanger has larger channels which do not allow water clogging to occur, consequently, ice blockage at very low outdoor temperatures are also diminished.
4. Bigger channels also reduce pressure drop, ease the cleaning of the heat exchanger and allow us to use lower density filters.
5. Yearly energy consumption, including the regained heat (by using the optimum heat exchanger) and night cooling, is calculated.

Experiment

1. Two airtight heat exchanger' models are made. The difference between the two is the size of heat exchanging channels. The both models are tested under two different climate conditions by using three separate flow rates. Temperature is measured at four ends of the models and ten thermocouples are distributed throughout the heat exchangers' length. The results show very close values between the measured and calculated efficiencies. The tested heat transfer coefficients are also very close to the calculated ones.
2. Due to an unevenly distributed air flow through the cross-section of the heat exchanger models, the temperature values measured by the thermocouples, though following the expected trends, are not that close to the estimated values.
3. Since the models are made manually, higher pressure drops occurred. They are not included in the results section.

Year Round Energy Consumption Calculation Using Wind Cowl

1. The wind cowl which is shown in figure 6-1 is chosen as the best performing cowl.
2. Due to a relatively high ductwork pressure drop, only 8% of energy is saved using the wind cowl in cold season. In warm season, however, due to high air flow rates and the cowl's resistance, more energy is required if the wind cowl is used. Summing up, the total yearly energy use, though negligibly, is increased when the wind cowls is used.

3. Two boundary cases of wind cowl performance are investigated. The simulation results are not sensitive to different assumptions under boundary conditions at high duct velocities (for further explanation see section 7).

Chapter 9

Recommendations

This is a wide range research, concerning three different subjects: ventilation, heat transfer and wind energy. Therefore, due to time constrains, a number of assumptions are made. A number of recommendations are made in return. They are divided into two groups: recommendations for ventilation and those for heat transfer.

Ventilation

1. The required maximum air flow rates are calculated for the whole dwelling. However, air flow distribution between the separate floors and rooms should be investigated according to the dwellers' location. Higher flow rates should be delivered to the bedrooms during the night, whereas larger air flow rates are needed in the living room in the day time. By doing so, the system's performance would increase even further.

2. In this research, it is assumed that the occupants are always present in the dwelling. In reality, of course, it is not always the case. Therefore, in order to reduce electricity control even further, flow rates for carbon dioxide control should be determined by using CO_2-sensors per room.

3. The 'Tussenwoning' type house characteristics are calculated by using the house layout (see fig. 3-1). But, many assumptions are made in order to simplify calculations, e.g. wall thickness, floors and ceilings are assumed to have the same thermal mass as the walls, the furniture thermal mass is ignored, window and door sizes are estimated etc. Therefore, the house parameters needed for a heat balance should be calculated by using more sophisticated methods.

4. As it has already been said, the night cooling control system forecasts temperature 11 hours ahead. This number is assumed. In order to check whether it is the optimum time span for the forecast of outdoor temperature, extra simulations should be done.

5. Night cooling begins to work if the forecasted temperature reaches a certain value. This value depends on the maximum flow rate, house characteristics and solar shading options. By knowing these variables, an approximate temperature value is chosen, however, the exact value should be found in further research.

Heat transfer

1. Heat exchange efficiency is calculated only for sensible heat. Yet, further calculations should also include latent heat. This is especially important if a heat exchanger is located in a very humid environment, e.g. greenhouses.

2. In order to differentiate temperature between different floors (or even rooms), separate versions of heat exchanger's which could be placed between the base and first floors, should be designed. Heat exchangers dimensions should be adjusted to the wanted temperature difference between the floors.

3. The size of heat exchanger channels are assumed. It is known that when the size of the channels decreases, the heat exchange coefficient increases. On the other hand, due to capillary forces, water can block the channels if their size is too little. Because of that, the exact size of the channels should be determined, such that they would not be blocked and have the highest possible heat exchange efficiency.

4. As it was mentioned at the beginning of chapter 2, air density is assumed to be constant. However, in future research, air density should be determined separately for every time period of the heating season.

Appendix A

House Characteristics Calculations

The windows', walls', roof's surface areas, the air and walls' volumes of the house are estimated using the dimensions given in figure 3-1 and mathematical expressions. Firstly, the house characteristics of every level is calculated. Then the calculated values of the different levels are added up. Figures A-1, A-2, A-3 and A-4 shows how the house (figure 3-1) is divided into four levels.

Base Level Calculations

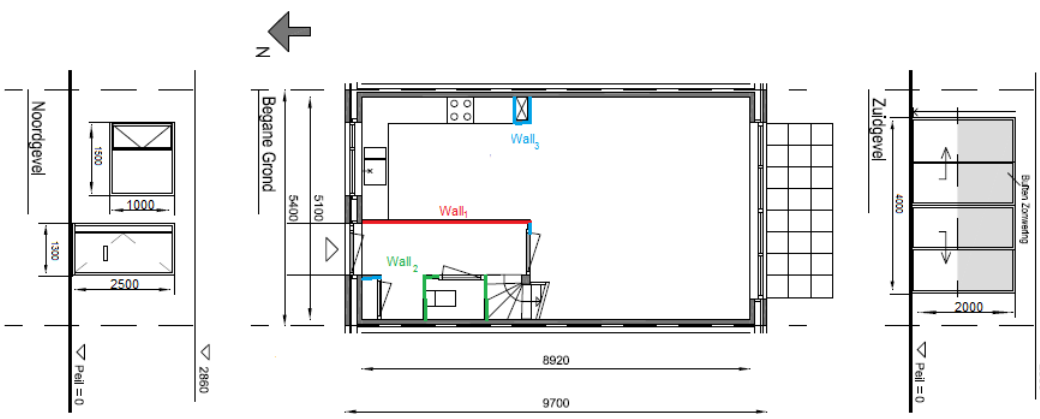

Figure A-1: House base level

$$A_{\text{windows0}} = A_{\text{north window}} + A_{\text{door}} + A_{\text{south window}} = 1.5m*1m + 2.5m*1.3m + 4m*2m = 12.75m^2 \quad \text{(A-1)}$$

$$A_{\text{walls+windows0}} = 2*A_{\text{north wall}} + 2*A_{\text{side wall}} = 2*5.4m*2.86m + 2*9.7m*2.86m = 86.37m^2 \quad \text{(A-2)}$$

$$A_{\text{walls0}} = A_{\text{walls+windows0}} - A_{\text{windows0}} = 73.6m^2 \quad \text{(A-3)}$$

$$A_{\text{inside walls0}} = A_{\text{wall 1}} + A_{\text{wall 2}} + A_{\text{wall 3}} = 4m*2.86m + 1.3m*2.86m + 2m*2.86m = 20.9m^2 \tag{A-4}$$

$$A_{\text{floor0}} = 5.1m * 8.92m = 45.5m^2 \tag{A-5}$$

$$V_{\text{walls+floor0}} = A_{\text{walls0}} * 0.1m + A_{\text{floor0}} * 0.1m = 12m^3 \tag{A-6}$$

$$V_{\text{inside walls0}} = A_{\text{inside walls0}} * 0.05m = 1.1m^3 \tag{A-7}$$

Note: Inside walls are multiplied by half of the thickness since it is assumed that indoor walls are thinner.

$$V_{\text{inside air0}} = 5.1m * 8.92m * 2.86m = 130m^3 \tag{A-8}$$

First Level Calculations

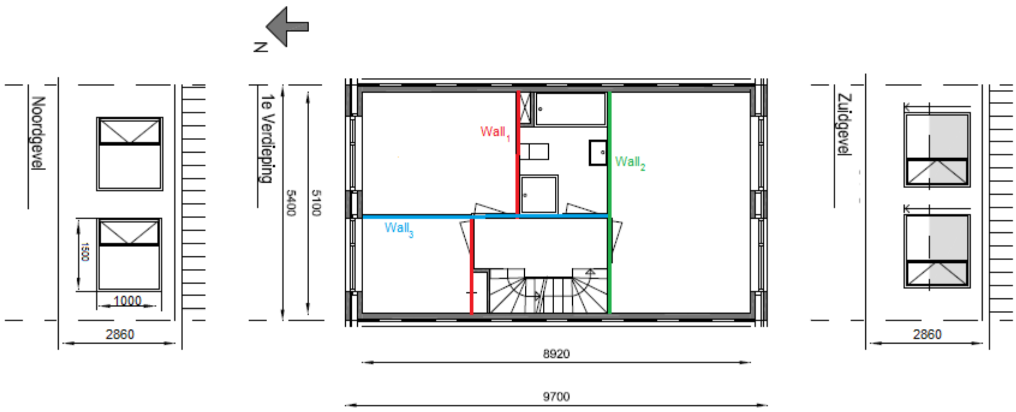

Figure A-2: House first level

$$A_{\text{windows1}} = 2*A_{\text{north window}} + 2*A_{\text{south window}} = 2*1.5m*1m + 2*1.5m*1m = 6m^2 \tag{A-9}$$

$$A_{\text{walls+windows1}} = 2*A_{\text{north wall}} + 2*A_{\text{side wall}} = 2*5.4m*2.86m + 2*9.7m*2.86m = 86.37m^2 \tag{A-10}$$

$$A_{\text{walls1}} = A_{\text{walls+windows1}} - A_{\text{windows1}} = 80.37m^2 \tag{A-11}$$

$$A_{\text{inside walls1}} = A_{\text{wall 1}} + A_{\text{wall 2}} + A_{\text{wall 3}} = 5.1m*2.86m + 5.1m*2.86m + \frac{2}{3}*8.92m*2.86 = 46.2m^2 \tag{A-12}$$

$$A_{\text{floor1}} = 5.1m * 8.92m = 45.5m^2 \tag{A-13}$$

$$V_{\text{walls1}} = A_{\text{walls1}} * 0.1m = 8m^3 \tag{A-14}$$

$$V_{\text{inside walls1}} = A_{\text{inside walls1}} * 0.05m + A_{\text{floor1}} * 0.1m = 6.86m^3 \tag{A-15}$$

$$V_{\text{inside air1}} = 5.1m * 8.92m * 2.86m = 130m^3 \tag{A-16}$$

Second Level Calculations

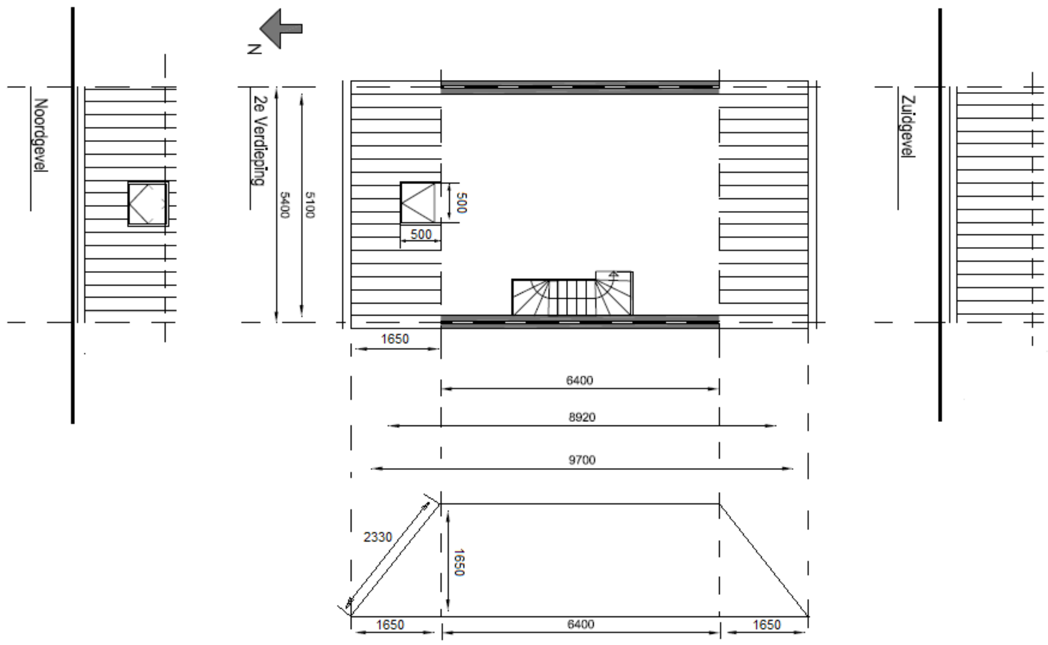

Figure A-3: House second level

$$A_{\text{window2}} = A_{\text{north window}} = 0.5m * 0.5m = 0.25m^2 \tag{A-17}$$

$$A_{\text{walls2}} = 2*A_{\text{side wall rectangle part}}+4*A_{\text{side wall triangle part}} = 2*6.4m*2.86m+4*(1.65m*1.65m)/2 = 26.5m^2 \tag{A-18}$$

$$A_{\text{ceiling2}} = 6.4m * 5.1m = 32.6m^2 \tag{A-19}$$

$$A_{\text{floor2}} = 8.92m * 5.1m = 45.5m^2 \tag{A-20}$$

$$V_{\text{walls2}} = A_{\text{walls2}} * 0.1m + A_{\text{ceiling2}} * 0.1m = 5.9m^3 \tag{A-21}$$

$$V_{\text{floor2}} = A_{\text{floor2}} * 0.1m = 4.6m^3 \tag{A-22}$$

$$V_{\text{inside air2}} = 2 * 5.1m * (1.65m * 1.65m)/2 + 6.4m * 5.1m * 1.65m = 67.7m^3 \tag{A-23}$$

$$A_{\text{roof2}} = A_{\text{total roof area}} - A_{\text{window2}} = 2 * 2.33m * 5.4m - 0.25m^2 = 25m^2 \tag{A-24}$$

Roof Level Calculations

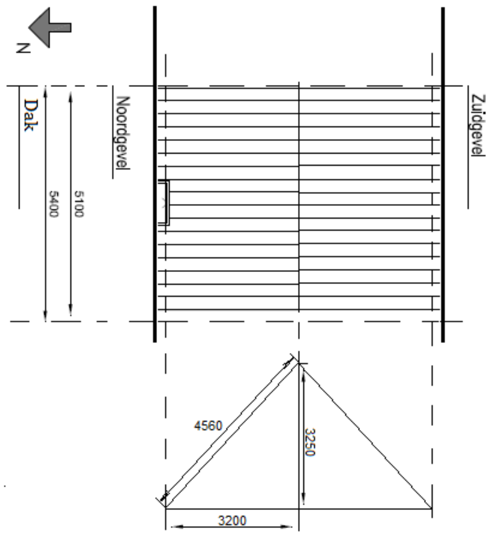

Figure A-4: House roof top

$$A_{\text{roof3}} = 2 * 4.56m * 5.4m = 49.3m^2 \tag{A-25}$$

Note: It is assumed that second level ceilings has same insulation as outside walls therefore the roof top is not included into air, wall volume and wall area calculations.

Envelope Area Calculations

$$A_{\text{norther+southern walls}} = 2 * 5.4m * 5.72m = 62m^2 \tag{A-26}$$

$$A_{\text{eastern+western walls}} = 2 * (8.92m * 5.72m + (4.9m * 4.85m/2)) = 126m^2 \tag{A-27}$$

$$A_{\text{roof}} = A_{\text{roof2}} + A_{\text{roof3}} = 74m^2 \tag{A-28}$$

$$A_{\text{envelope}} = A_{\text{norther+southern walls}} + A_{\text{eastern+western walls}} + A_{\text{roof}} = 262m^2 \tag{A-29}$$

Final Calculations

$$A_{\text{windows}} = A_{\text{windows0}} + A_{\text{windows1}} + A_{\text{window2}} = 19m^2 \tag{A-30}$$

$$A_{\text{walls}} = A_{\text{walls0}} + A_{\text{walls1}} + A_{\text{walls2}} = 180m^2 \tag{A-31}$$

$$V_{\text{inside air}} = V_{\text{inside air0}} + V_{\text{inside air1}} + V_{\text{inside air2}} = 328m^3 \tag{A-32}$$

$$V_{\text{walls}} = V_{\text{walls+floor0}} + V_{\text{walls1}} + V_{\text{walls+ceiling2}} = 25.9m^3 \tag{A-33}$$

$$V_{\text{inside walls}} = V_{\text{inside walls0}} + V_{\text{inside walls1}} + V_{\text{floor2}} = 12.5m^3 \tag{A-34}$$

Appendix B

Comparison of two Studies Results Concerning Needed Flow Rates

In figure B-1, required ventilation flow rates for humidity control in the Netherlands is shown. Threshold of relative humidity is 90%. Figure B-2 represents the required flows which are found in this study. Threshold of relative humidity is 90%.

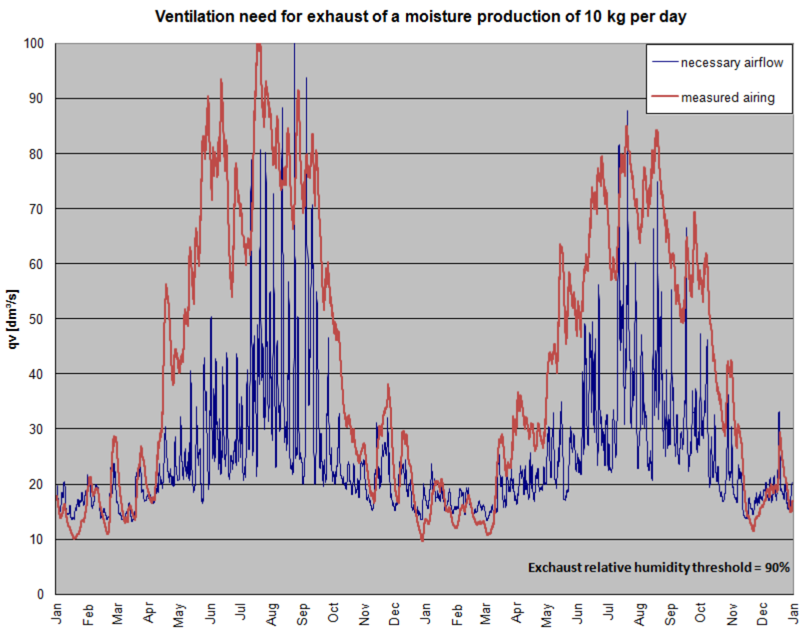

Figure B-1: Required ventilation flow rates for the humidity control according to TNO research

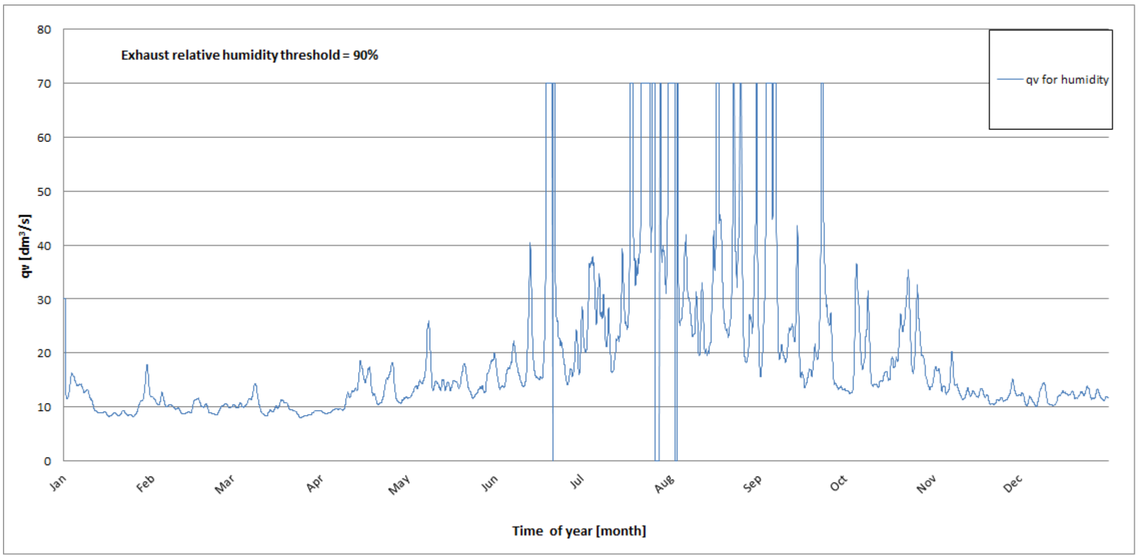

Figure B-2: Required ventilation flow rates for humidity control according to this study

Appendix C

Heat Exchanger Models Comparison

qv=30 (dm^3/s)					
		MODEL_1	MODEL_2	MODEL_3	MODEL_4
Cost (€):	**TOTAL**	**4361**	**5126**	**4335**	**4113**
	electricity_winter	78	61	108	108
	electricity_summer	1382	1380	1665	1404
	lost heat	1404	2309	975	975
	material	861	739	951	966
	space	636	636	636	660
Dimensions (m):	L	1	1	1	1
	D	0.3	0.3	0.3	0.3
	H_elements	0.01	0.01	0.01	0.01
Parameters:	dP_winter (Pa)	31	25	44	44
	dP_summer(Pa)	127	126	178	131
	Efficiency (%)	69	49	79	79
	HE_cross-section(m2)	0.0392	0.0419	0.0375	0.0375
	heat_exchange_area(m2)	15.1	8.1	21.6	21.6

Table C-1: Comparison of four models, qv=30 dm^3/s

Appendix D

Wind Cowls and Openings

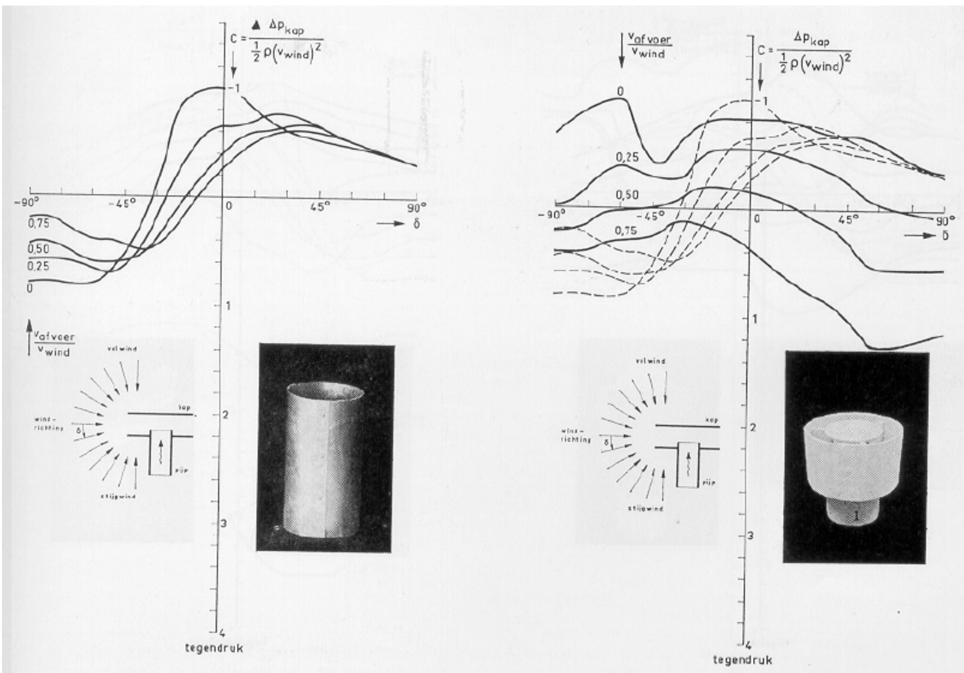

Figure D-1: Wind cowls: Nr. 1 (left), Nr. 2 (right)

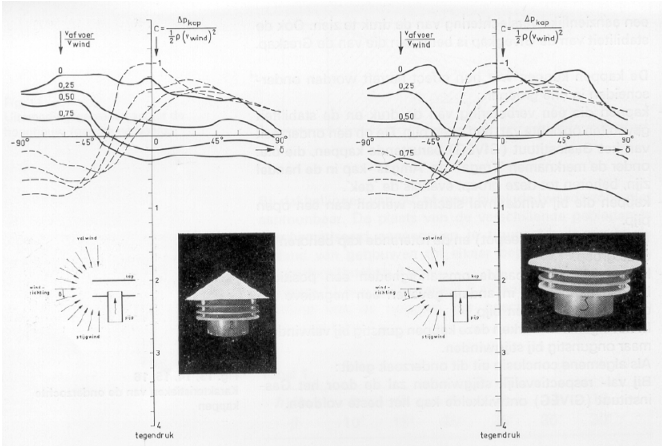

Figure D-2: Wind cowls: Nr. 3 (left), Nr. 4 (right)

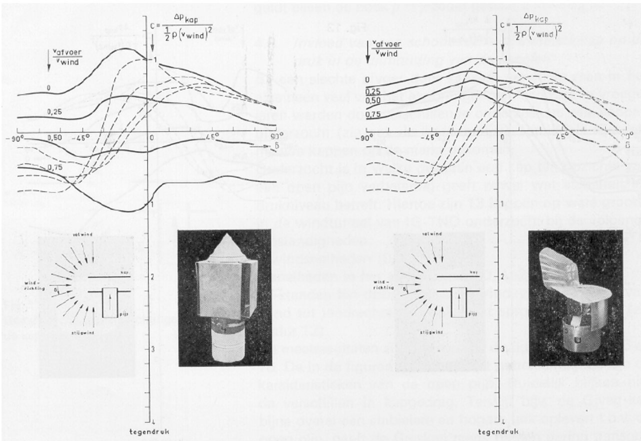

Figure D-3: Wind cowls: Nr. 5 (left), Nr. 6 (right)

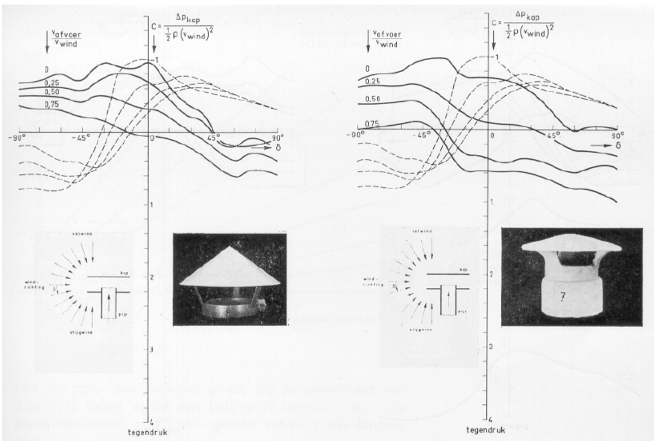

Figure D-4: Wind cowls: Nr. 7 (left), Nr. 8 (right)

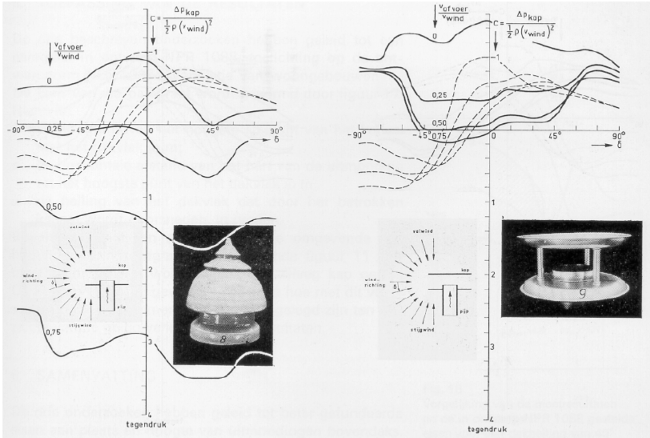

Figure D-5: Wind cowls: Nr. 9 (left), Nr. 10 (right)

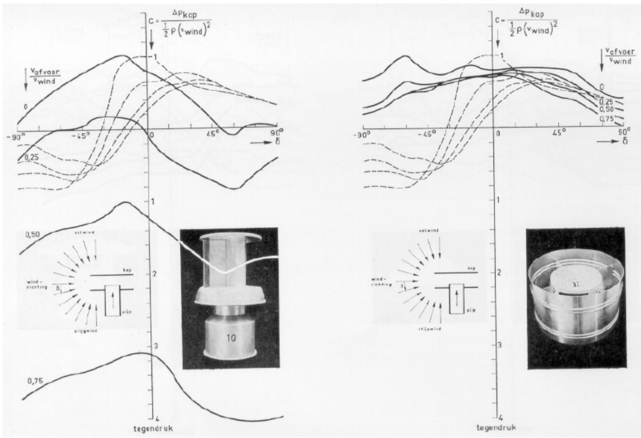

Figure D-6: Wind cowls: Nr. 11 (left), Nr. 12 (right)

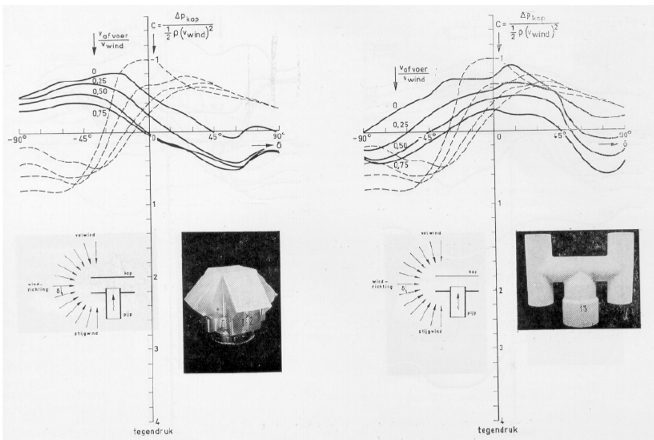

Figure D-7: Wind cowls: Nr. 13 (left), Nr. 14 (right)

Appendix E

Experiment Pictures

Figure E-1: Two heat exchangers, insulated and prepared for testing

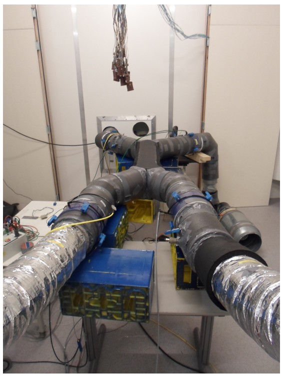

Figure E-2: Heat exchanger test in climate chamber

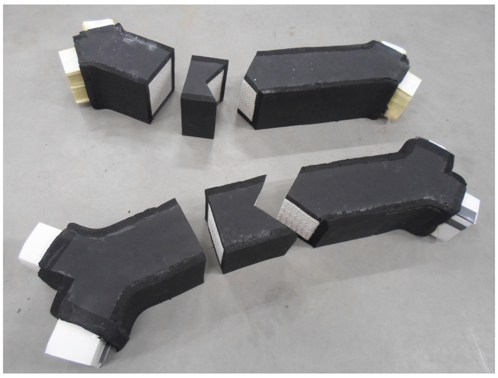

Figure E-3: After testing. Cut heat exchangers

Figure E-4: After testing. Different channel size of both heat exchangers

Bibliography

[1] Organisation for Economic Co-operation and Development/International Energy Agency, "Energy balances of oecd countries 1991-1992," *Paris*, France 1994.

[2] Kohonen R., "Energy conservation in builidng and community systems - strategy plan 1994-97," *International Energy Agency BCS Implementing Agreement*, 1994.

[3] W. Passchier-Vermeer, "Milieu en gezondheid: overzicht van risico's doelen en beleid," *TNO Preventie en Gezondheid. Leiden*, TNO-rapport PG/VGZ/2001.95. 2001.

[4] E. H. Jan van Ginkel, "Indoor air quality influenced by ventilation system design," *The Residential Context of Health*, July 2006.

[5] Centers for Disease Control and Prevention and U.S. Department of Housing and Urban Development, *Healthy Housing Reference Manual.* U.S. Department of Health and Human Services, 2006.

[6] WHO Regional Office for Europe, *Air Quality Guidelines for Europe.* 2nd ed. Copenhagen, 2000.

[7] The WHO European Centre for Environment and Health, *WHO Guidelines for Indoor Air Quality: Selected Pollutants.* Bonn Office, 2010.

[8] Air Infiltration and Ventilation Center, *A Guide to Energy Efficient Ventilation.* International Energy Agency, 1996.

[9] C.P. Yaglou and W.N. Witheridge, "Ventilation requirements," *ASHRAE Trans*, 1937.

[10] P. O. Fanger, "New principles for a future ventilation standard," *Proc Indoor Air*, 1993.

[11] P. O. Fanger, "Introduction of the olf and the decipol units to quantify air pollution perceived by humans indoors and outdoors," *Energy and buildings*, No 12 1988.

[12] H. Bouwman, "Minimum ventilation rates," *Report C 470E*, IMG-TNO 1983, Delft.

[13] A.C. Van der Linden, "Bouwfysica," *Spruyt, Van Mantgem De Does BV*, Leiden 1996.

[14] "The Engineering ToolBox." http://www.engineeringtoolbox.com/met-metabolic-rate-d_733.html. Accessed: 10/10/2014.

[15] W. Gids, "Ventilatie van ruimten ten behoeve van personen," *TNO-rapport*, February 22 2011.

[16] American Society of Heating, Refrigerating and Air-Conditioning Engineers, Inc., "Ventilation for acceptable indoor air quality," *ANSI/ASHRAE Standard 62-2001*, 2003.

[17] J. Lstiburek, "Relative humidity," *Building Science Corporation*, April 2002, Westford.

[18] T.D. Brock and M.T. Madigan, "Biology of micro-organisms," *Prentice Hall int. 5th ed.*, 1988.

[19] T. E. Mull, *HVAC: Principles and Applications Manual.* McGraw- Hill, New York, 1997.

[20] C. Gilmore, "More comfort for your heating dollar," *Popular Science:99*, September 1972.

[21] A. Boeke, "Inleiding tot de luchtbehandelingstechniek; automatische regeling van luchtbehandelingsinstallaties," *georganiseerd door het Koninklijk Instituut van Ingenieurs*, oktober 1967.

[22] Rotronic, *The Rotronic Humidity Handbook.* Rotronic Instrument Corp., 2005.

[23] A.K. Raue, S.R. Kurvers, A.C. van der Linden, A.C. Boerstra, W. Plokker, "Dutch thermal comfort guidelines: from weighted temperature exceeding hours towards adaptive temperature limits,"

[24] P.O. Fanger, *Thermal Comfort, Analyses and Aplications in Environmental Engineering.* McGraw-Hill, London, New York, 1970.

[25] R. de Dear, G. Brager, D. Cooper, "Developing an adaptive model of thermal comfort and preference," *Final report, ASHRAE RP/884*, 1997.

[26] International Standard: ISO 13790:2008 (E), *Energy Performance of Buildings - Calculation of Energy Use for Space Heating and Cooling.* 2008.

[27] Sadik Kakac, Hongtan Liu, *Heat exchangers, selection, rating, and thermal design.* CRC PRESS, 2002.

[28] L.P.B.M. Janssen, M.M.C.G. Warmoeskerken, *Transport Phenomena Data Companion.* VSSD, The Netherlands, 2006.

[29] H. Recknagel, E-R. Schramek, E. Sprenger, *Taschenbuch fur Heizung + Klima Technik*. R. Oldenbourg Verlag Munchen Wien, 1999.

[30] J.F. Manwell, J.G. McGowan, A.L. Rogers, *Wind Energy Explained, Theory, Design and Application*. Wiley, 2002.

[31] T. Burton, D.Sharpe, N. Jenkins, E. Bossanyi, *Wind Energy Handbook*. Wiley, 2001.

[32] S. Toet, "Energieproductie uit wind gedreven ventilatie," *Delft University of Technology*, 2002.

[33] W.F. de Gids, L. den Ouden, "Drie onderzoeken naar de werking van kanalen voor naturlijke ventilatie, waarbij nagegaan is de invloed van plaats en hoogte van de uitmonding, van de bebouwing in de omgeving en van de vorm van de uitmonding," *UDC 533.6.07*.

[34] A. W. Andreas Pfeiffer, Viktor Dorer, "Modelling of cowl performance in building simulation tools using experimental data and computational fluid dynamics," *Building and Environment 43, 1361-1372*, Elsevier 2008.

[35] Ministerie van Binnenlandse Zaken en Koninkrijksrelaties, "Voorbeeldwoningen 2011, bestaande bouw. als het gaat om energie en klimaat," 2011.

[36] British Cement Association, "Foamed concrete composition and properties," 1994.

[37] "Your home, australia's guide to environmentally sustainable homes." http://www.yourhome.gov.au/materials/precast-concrete. Accessed: 16/11/2014.

[38] "Online Bouwbesluit." http://www.onlinebouwbesluit.nl/l. Accessed: 20/10/2014.

[39] J.T. van Ginkel, E. Hasselaar, "Goede ventilatie beperkt schimmelrisico in badruimte," *TVVL Magazine*, April 2008.

[40] J. van Dongen, "Gezondheidsaspecten van woningen in nederland," *Ministerie van VROM*, TNO-rapport 2007.

[41] "Internal research of TNO." Accessed: 5/9/2014.

[42] A.C. van der Linden, "Zonwering," *Kennisbank Bouwfysica*, augustus 2005.

[43] Vereniging Leveranciers van Luchttechnische Apparaten, "Vla-methodiek gelijkwaardigheid voor energiebesparende ventilatieoplossingen in woningen," *Zoetermeer, versie 1.1*, Mei 2013.

[44] S. ter Mors, J.L.M. Hensen, M. Loomans, A. Boerstra, "Adaptive thermal comfort in primary school classrooms: Creating and validity pmv - based comfort charts," *Building and Environment*, 46 (12), pp. 2454 - 2461 2011.

[45] "The fluctuations in temperature in The Netherlands." http://www.windfinder.com/windstatistics/hoek_van_holland. Accessed: 16/04/2014.

[46] "Eurostat, Electricity prices by the type of user." http://ec.europa.eu/eurostat/tgm/refreshTableAction.do?tab=table&plugin=1&pcode=ten00117&language=en. Accessed: 10/01/2015.

[47] "ePlastics, ridout plastics." http://www.eplastics.com/PETG_Vivak. Accessed: 12/01/2014.

[48] "Rules of thumb from the tno building department." TNO. Accessed: 7/1/2015.

[49] K.S. Sutherland, G. Chase, *Filters and Filtration Handbook*. Elsevier, 1997.

[50] "TNO database, pressure drop calculation for the optimized ductwork." Accessed: 15/04/2015.

[51] "Mollier Sketcher 2.1, beta." http://mollier-sketcher.software.informer.com/2.1b/. Accessed: 10/01/2014.